The Plant Cell, Vol. 20: 947–968, April 2008, www.plantcell.org © 2008 American Society of Plant Biologists

Distinct Light-Initiated Gene Expression and Cell Cycle Programs in the Shoot Apex and Cotyledons of *Arabidopsis* [W]

Enrique López-Juez,[a,1] Edyta Dillon,[a,2] Zoltán Magyar,[a,b] Safina Khan,[a] Saul Hazeldine,[c,3] Sarah M. de Jager,[d] James A.H. Murray,[d] Gerrit T.S. Beemster,[e,f] László Bögre,[a] and Hugh Shanahan[c]

[a] School of Biological Sciences, Royal Holloway, University of London, Egham, Surrey TW20 0EX, United Kingdom
[b] Institute of Plant Biology, Biological Research Center, H-6701 Szeged, Hungary
[c] Department of Computer Science, Royal Holloway, University of London, Egham, Surrey TW20 0EX, United Kingdom
[d] Institute of Biotechnology, University of Cambridge, Cambridge CB2 1QT, United Kingdom
[e] Department of Plant Systems Biology, Flanders Institute of Biotechnology, B-9052 Gent, Belgium
[f] Department of Molecular Genetics, Gent University, B-9052 Gent, Belgium

In darkness, shoot apex growth is repressed, but it becomes rapidly activated by light. We show that phytochromes and cryptochromes play largely redundant roles in this derepression in *Arabidopsis thaliana*. We examined the light activation of transcriptional changes in a finely resolved time course, comparing the shoot apex (meristem and leaf primordia) and the cotyledon and found >5700 differentially expressed genes. Early events specific to the shoot apices included the repression of genes for Really Interesting New Gene finger proteins and basic domain/leucine zipper and basic helix-loop-helix transcription factors. The downregulation of auxin and ethylene and the upregulation of cytokinin and gibberellin hormonal responses were also characteristic of shoot apices. In the apex, genes involved in ribosome biogenesis and protein translation were rapidly and synchronously induced, simultaneously with cell proliferation genes, preceding visible organ growth. Subsequently, the activation of signaling genes and transcriptional signatures of cell wall expansion, turgor generation, and plastid biogenesis were apparent. Furthermore, light regulates the forms and protein levels of two transcription factors with opposing functions in cell proliferation, E2FB and E2FC, through the Constitutively Photomorphogenic1 (COP1), COP9-Signalosome5, and Deetiolated1 light signaling molecules. These data provide the basis for reconstruction of the regulatory networks for light-regulated meristem, leaf, and cotyledon development.

INTRODUCTION

Light is a key environmental cue controlling plant development. The dramatic influence of light on plant development can be seen when, after germination, young seedlings undergo a transition from dark growth (skotomorphogenesis) to light growth (photomorphogenesis). Skotomorphogenesis, or etiolated growth, involves rapid hypocotyl elongation, slow root growth, a closed apical hook in the hypocotyl, folded and unexpanded cotyledons with cells containing proplastids or etioplasts, and an arrested shoot apical meristem. Upon light irradiation, seedling development is switched to an alternative developmental program whereby hypocotyl elongation is reduced, the apical hook opens, cotyledons unfold, their cells expand, their plastids differentiate into chloroplasts, and the shoot apical meristem initiates the development of true leaves (Whitelam and Halliday, 2007). An important feature of photomorphogenesis is that the same light signal evokes largely different and sometimes opposite responses in different cells, tissues, and organs (e.g., cell division and growth in the shoot apical meristem, largely cell expansion–driven growth in the cotyledons, and repression of growth in the hypocotyl). How these distinct tissue-specific responses are achieved has begun to be addressed by analyzing the complementary growth responses of hypocotyls and cotyledons (Ma et al., 2002; Khanna et al., 2006). Surprisingly, in spite of their central importance to adult plant growth, we know little about the light-mediated derepression of shoot meristem activity and leaf development and about light-induced chloroplast differentiation in cotyledons and leaves.

Light initiates photomorphogenesis through the action of photoreceptors. Plant photoreceptors include the phytochrome, cryptochrome, phototropin, and other light/oxygen/voltage domain–containing protein families (reviewed in Whitelam and Halliday, 2007). While phytochromes perceive light most effectively in the red/far-red region of the spectrum, cryptochromes and phototropins detect blue and UV-A light. Photomorphogenesis is primarily determined by the combined action of phytochromes and cryptochromes, since these two families of photoreceptors are responsible for the vast majority of the gene expression changes that occur in seedlings upon first light exposure (Ma et al., 2001; Ohgishi et al., 2004). Different phytochromes have

[1] Address correspondence to e.lopez@rhul.ac.uk.
[2] Current address: St. George's, University of London, Cranmer Terrace, London SW17 0RE, UK.
[3] Current address: Department of Computational and Systems Biology, John Innes Centre, Norwich Research Park, Colney, Norwich NR4 7UH, UK.
The author responsible for distribution of materials integral to the findings presented in this article in accordance with the policy described in the Instructions for Authors (www.plantcell.org) is: Enrique López-Juez (e.lopez@rhul.ac.uk).
[W] Online version contains Web-only data.
www.plantcell.org/cgi/doi/10.1105/tpc.107.057075

subtly distinct roles, for example, in the control of leaf versus internode growth (Whitelam and Halliday, 2007).

In a search for genes that maintain the skotomorphogenesis program, a number of *deetiolated* (*det*) and *constitutively photomorphogenic* (*cop*) mutants have been identified (Chory et al., 1989; Deng et al., 1991). These mutants undergo photomorphogenesis even when grown in the total absence of light: the shoot meristem remains active, and the *det1-1* and *cop1-4* mutants can form rosette leaves in the dark, although some other *cop* and *det* mutants are seedling-lethal (Moller et al., 2002). The molecular functions for many of these mutants have been identified. The *cop9* mutant has led to the discovery of a protein complex, the COP9 (for Constitutively Photomorphogenic9) signalosome (CSN), that is homologous with the proteasome lid and functions in targeted proteolysis, primarily as a regulator of the SCF-type E3 ubiquitin ligase complexes (Sullivan et al., 2003; Wei and Deng, 2003). COP1 is a Really Interesting New Gene (RING) finger protein with E3 ubiquitin ligase activity. These mutants have uncovered a common theme in light signaling: the targeted proteolysis of positive regulators in the dark and the specific inactivation of these proteolysis mechanisms by light. The best characterized target of the COP1- and CSN-mediated proteolysis is Elongated Hypocotyl5 (HY5) (Osterlund et al., 2000), a transcription factor of the basic domain/leucine zipper (bZIP) class. Both COP1 and CSN are conserved in eukaryotes. In animal cells, during *Drosophila* oogenesis, CSN was found to function in the regulation of cell proliferation (Doronkin et al., 2003).

Microarray analysis has been used extensively to understand the transcriptional program of plant light responses (Jiao et al., 2007). These experiments focused on the extent, diversity, and involvement of COP signal transducers (Ma et al., 2001), the early responses and their sensors (Tepperman et al., 2001, 2004; Ohgishi et al., 2004), or the differential organ response (Ma et al., 2005). Whole-genome transcriptome analysis of leaf development has also been performed, starting from young leaf primordia <3 mm long, and has uncovered the gene expression program associated with the arrest of cell division (Beemster et al., 2005).

In plants, the growth of new organs, such as leaves, takes place primarily in or near meristems. This requires a combination of cell division, cell growth, morphogenesis, cell expansion, and differentiation. The Retinoblastoma (RB) pathway plays an important role in regulating these events in plants and animals (Du and Pogoriler, 2006; Fleming, 2006; De Veylder et al., 2007; Timmers et al., 2007). The RB family of proteins controls the activity of E2F transcription factors and globally represses promoters by recruiting chromatin-remodeling enzymes. RB function is inactivated through hyperphosphorylation by the cyclin-dependent protein kinase in complex with D-type cyclins (Du and Pogoriler, 2006). In *Arabidopsis thaliana*, *Retinoblastoma-Related1* (*RBR1*) is the single homolog of *RB*, while there are three *E2F*-related genes performing different functions: *E2FC* is a transcriptional repressor (del Pozo et al., 2006), whereas *E2FA* and *E2FB* are activators (De Veylder et al., 2002; Magyar et al., 2005). Most likely, RBR1 regulates all three E2Fs, and these control plant cell cycle and differentiation through poorly understood mechanisms.

Light provides an easy-to-manipulate environmental switch for the state of shoot meristem activity and can help to address fundamental questions in meristem function. In this work, we first established that meristem activity and cell cycle progression are fully under photoreceptor control, monitoring multiple *Arabidopsis* mutants defective in phytochromes and cryptochromes. We then used microarray profiling of global gene expression changes during photomorphogenesis in apical tissue and cotyledons separately. These data provide a novel resource with high spatial and temporal resolution and, importantly, with a specific off/on environmental switch condition. We found that in dark-grown shoot apices, genes coding for components in regulated proteolysis, signaling, and specific groups of transcription factors are expressed but become rapidly downregulated by light exposure. Light initiates several hormonal responses associated with meristem function, particularly those of auxin and ethylene (negative) and cytokinin and gibberellin (GA; positive). Light further triggers rapid cell growth/protein translation and a coordinated progression through the cell cycle, which is instigated in a manner consistent with regulation of the abundance of two central cell cycle regulators, the E2FB and E2FC transcription factors, partly via COP1, DET1, and the CSN. Our analysis lays the foundation to identify biologically important individual growth phenomena, some of their molecular switches as well as integrators among them, and may help to build a network of elementary processes underlying the development of leaves.

RESULTS

Photoreceptors Function in an Overlapping Manner to Repress Meristem Activity

In order to examine which photoreceptors are responsible for the control of meristem activity, we generated mutants with combinatorial defects in multiple phytochromes and cryptochromes. Mazzella and coworkers (2001) reported a severe deetiolation defect in *phyA phyB cry1 cry2* (for *phytochrome A phytochrome B cryptochrome1 cryptochrome2*) quadruple mutants, although the leaf initiation phenotypes of mutant combinations were not examined. Since multiple phytochrome apoproteins share one chromophore, phytochromobilin, we used the *hy1* mutant, which is defective in the main heme oxygenase and, as a result, unable to synthesize the bulk of phytochromobilin (Muramoto et al., 1999). Hypocotyl elongation, as was known previously, is primarily controlled by phytochromes and cry1 in a redundant manner (Figure 1A). *hy1* plants also displayed a reduced number of rosette leaves at the 19-d stage, as a result of delayed leaf production compared with the wild type or with mutants in *cry1*, *cry2*, or both cryptochromes (Figure 1B). However, the redundant roles of cryptochromes in meristem activation become apparent through the much more severe deetiolation phenotypes of plants defective in multiple phytochromes and both cryptochromes, compared with plants with none or only one of the cryptochromes mutated (Figure 1B). Examination of the shoot apical meristem in the wild type demonstrated the arrested meristem in the dark and the rapidly resumed growth of primordia upon transfer to light, with leaf primordia showing differentiating trichomes as rapidly as after 2 d (Figure 1C). Again, the multiple phytochrome and cryptochrome mutant exhibited extreme delay in the activation of leaf primordia growth in the light.

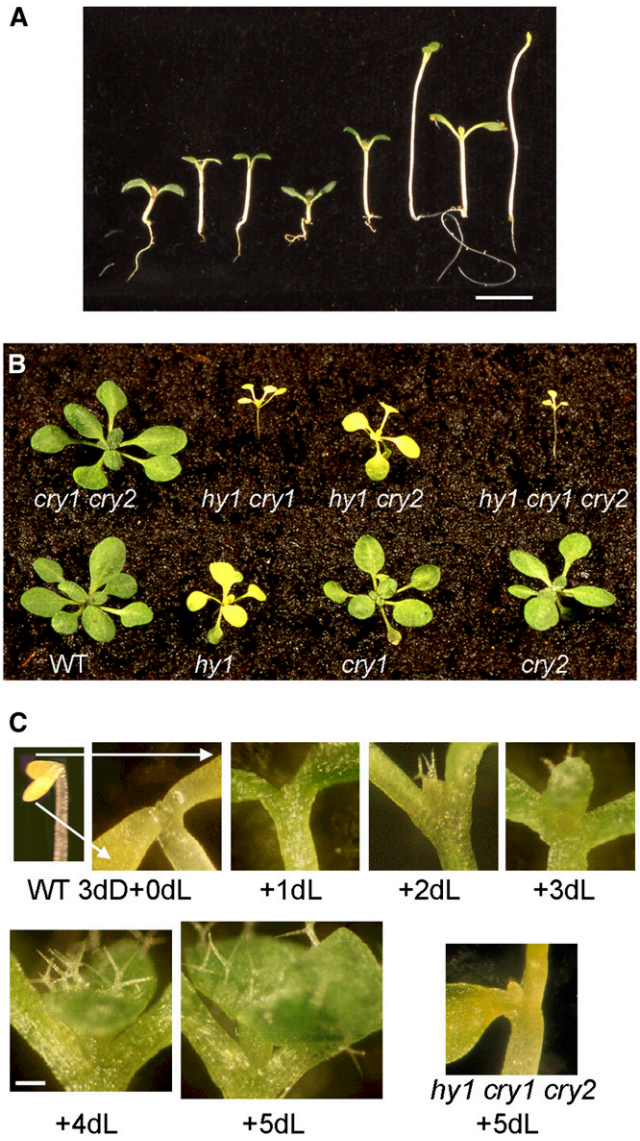

Figure 1. Phytochromes and Cryptochromes Redundantly Contribute to the Relief of the Dark Repression of Meristem Activity.

(A) Five-day-old seedlings of the following genotypes (from left to right) were grown on agar under white light: wild-type L*er*, *hy1*, *cry1*, *cry2*, *cry1 cry2*, *hy1 cry1*, *hy1 cry2*, and *hy1 cry1 cry2*. Bar = 5 mm.
(B) Soil-grown, 19-d-old plants of the same genotypes shown in **(A)**. The wild-type plant is 40 mm across.
(C) Close-up of the shoot apical region of Ler wild-type seedlings grown for 3 d in the dark (3dD), followed by a variable number of days in the light (+1dL to +5dL), and of a *hy1 cry1 cry2* seedling grown for 3dD+5dL. Bar for all close-ups = 250 μm.

Dynamic Light-Induced Transcriptional Responses in Dissected Shoot Apices and in Cotyledons during Deetiolation

The rapid and synchronous induction of growth in shoot apices when dark-grown seedlings are transferred to light offers an excellent experimental system in which to unravel the underlying gene expression program. We chose to compare genome-wide mRNA levels in dissected shoot apices, including the meristem and leaf primordia, with those of cotyledons, two seedling regions with distinct light responses. We reasoned that a large number of processes would take place in response to light in the shoot apex, including cell cycle activation, leaf organogenesis, chloroplast differentiation, and the production of photoprotectant flavonoids. Some of these processes would also be expected to take place in the cotyledons, while others, such as cell division, were anticipated to be different. Samples were taken at 0, 1, and 6 h after the transition from dark to light, separately for shoot apices and cotyledons, in biological duplicates in each case. Each sample contained material from at least 1500 seedlings (see Methods for details). We also collected single shoot apex samples, pooled from multiple experiments, at 24, 48, and 72 h after the light induction (see Supplemental Figure 1 online).

RNA was extracted and hybridized to the Affymetrix ATH1 GeneChip array that contains probes for nearly 23,000 *Arabidopsis* genes. Supplemental Figure 1 online outlines the procedures used in the experiment and in the analysis of the array data. The raw hybridization data were converted to normalized expression values using three independent strategies (see Methods). Quality control of RNA integrity on the data led us to hybridize one new, replacement sample (see Supplemental Figure 1A online). A hierarchical clustering tree of samples, and scatterplots of normalized expression values for individual genes between samples, confirmed the similarity between replicates and the spread when comparing different time points (see Supplemental Figures 1B and 1C online). Expression values for all genes (as determined by GC-content robust multi-array [gcRMA] normalization) are given in Supplemental Table 1 online.

We then generated a list of differentially expressed genes, using the samples and time points for which replicas were available (0, 1, and 6 h). Genes were selected based on a two-factor analysis of variance (ANOVA) applied onto the expression data generated by each of the three normalization methods, and a 5% false discovery rate was chosen to determine the threshold P value for differential expression in each case. Finally, a filter for a minimum twofold expression change was applied. A total of 5620 probes, representing 5794 genes, fulfilled these criteria and were subjected to further analyses. These genes, their individual and averaged expression values (gcRMA), and statistical parameters representing their fold change in shoot apices or cotyledons, at 1 or 6 h, are given in Excel format in Supplemental Table 2 online.

Identification of Coregulated Gene Clusters and Their Associated Biological Functions

The quest for biological themes used two parallel approaches. In the first, computational techniques identified groups of differentially expressed genes sharing similar expression kinetics (unsupervised clusters). In the second, differentially expressed genes were selected if they statistically followed one of a number of a priori chosen patterns of expression likely to be of relevance (supervised patterns). The latter included, for example, genes showing rapid change upon light exposure only in the shoot apex. In both cases, these clusters of genes were explored for

overrepresentation of biological functions as indicated by both functional classification and Gene Ontology (GO) terms. Finally, when a biological function was identified as strongly represented in a gene cluster, comprehensive lists of genes possessing that function were compiled and analyzed for their expression pattern in the complete experiment.

For the unsupervised gene clusters, the genes included in each cluster, and selected overrepresented GO terms for each cluster are shown in Figure 2A, Supplemental Table 2 online, and Table 1, respectively. Equivalent data for the supervised patterns are shown in Supplemental Figure 2 and Supplemental Tables 3 and 4 online. Finally, the gene composition of every cluster and supervised pattern is shown in detail in associated links available at http://www.cs.rhul.ac.uk/Plant-Systems-Biology.

Validation of the Apex- and Cotyledon-Specific Dynamic Gene Expression Patterns upon Light Induction by Quantitative Real-Time PCR

Quantitative real-time PCR (qPCR) was used to monitor selected genes whose expression was shown to change by the combined microarray data. The selection of genes also provided a first opportunity to validate the experimental setup used in the microarray experiment, in terms of monitoring previously known light responses, and in the ability to identify genes with very different expression patterns in the shoot apex and cotyledon samples. The latter confirms the distinct identity and thus the success in the dissection of these samples. The results are presented in Figure 3. The meristem-specific genes *Shoot Meristemless* (*STM*) and *Arabidopsis Knotted-like1* (*KNAT1*), associated with the discrimination of stem cell and differentiation domains, were expressed in cotyledon samples at levels that were, at most, 1% of those in the shoot apex samples. Conversely, genes for a thylakoid protein (At3g15110) and a cell wall peroxidase (PERX34) were expressed in cotyledons at levels between 3 and 12 times those in shoot apices, and Teosinte Branched1, Cycloidea, PCF-4 (TCP4) was expressed at levels at least 11 times those in shoot apex samples at the same time points. Contamination of cotyledon petioles and the hypocotyl hook is expected in shoot apex samples given the dissection procedure, but these tissues appeared to make only a small contribution. The shoot apex samples contained both the shoot apical meristem and the incipient leaf primordia. Although the primordia increased in size over the latter points (Figure 1C), such changes in tissue composition do not appear to have been responsible for substantial changes in gene expression. For example, *STM* (expressed in the meristematic central zone), *KNAT1* (expressed in the meristem peripheral zone but not in the leaf primordia), and *AS1* (At2g37630; expressed in the primordia) did not show consistent shifts in expression over the course of the experiment.

qPCR confirmed the expression changes of genes representing key processes, such as classic light-induced *Chalcone Synthase* or light-repressed *Protochlorophyllide Reductase A* genes, or genes involved in cell cycle, growth, and hormone action. Overall, for all 16 genes, the qPCR and microarray data extracted by the gcRMA normalization algorithm showed an average Pearson correlation coefficient of 0.874, indicating a high overall reliability of the array results. It was also apparent that the microarray values tended to underestimate the magnitude of the differences in expression. As an example, the meristem-specific genes showed on average >700-fold higher expression in shoot apices than in cotyledons according to qPCR data but only 58-fold higher expression according to the gcRMA-normalized array values.

To further validate our data, we compared them with the results obtained in earlier experiments using whole seedlings. A previous study, using the same ATH1 GeneChip, focused on early light responses and identified robustly red light–regulated genes within 1 h of light exposure (Tepperman et al., 2004). Supplemental Figure 3 online shows that a majority of these light-regulated genes have also been identified as differentially expressed in our analysis. Using a spotted oligomer microarray platform, another study analyzed the differential response to long-term light or dark growth in cotyledons, hypocotyls, or seedling roots (Ma et al., 2005). The proportion of shared genes identified by this analysis and ours was smaller, probably owing not only to the different platform but also to the long-term light exposure used by Ma and collaborators (2005) (see Supplemental Figure 3 online).

Gene expression patterns were also established by microdissection of cotyledons and the shoot meristem region during embryogenesis (Spencer et al., 2007). At the torpedo stage, only a few genes (49; see Supplemental Table 5 online) are shoot meristem–specific. These typically are expressed at low levels, and in our study only *STM* had an obvious shoot apex–specific expression. However, a large number of genes expressed in embryo cotyledons (722) are also present in the seedling cotyledon. Many of these genes encode ribosomal and chloroplast proteins, induced by light in shoot apical tissue and constitutively expressed in cotyledons (see Supplemental Figure 3C online).

Transcriptional Signatures Suggest Rapid Signaling Processes through Protein Turnover and Phosphorylation, Predominantly in the Shoot Apex

We sought transcriptional responses exclusive or quantitatively predominant to the shoot apex. Unexpectedly, the majority of such genes displayed a negative regulation by light (clusters 5 and 6 [Figure 2] and supervised downregulated patterns [see Supplemental Figure 2 online]). In all of these clusters and patterns, a significant proportion of genes were associated with zinc ion binding GO terms, including zinc finger–containing transcription factors and particularly RING zinc finger proteins with roles in ubiquitination and proteolysis and possibly the subcellular localization of associated proteins (Moller et al., 2002). Therefore, we monitored the entire family of these proteins. The results further underlined this coordinated, large-scale downregulation of genes for targeted proteolysis, many of them predominantly regulated in the shoot apex, where most of these changes were transient (Figure 4A; note the bottom cluster). The lists of genes in this and other gene families are presented, with their expression values, in Supplemental Table 5 online. Five genes for RING finger proteins underwent an eightfold or greater drop in expression within the first hour and were at least threefold

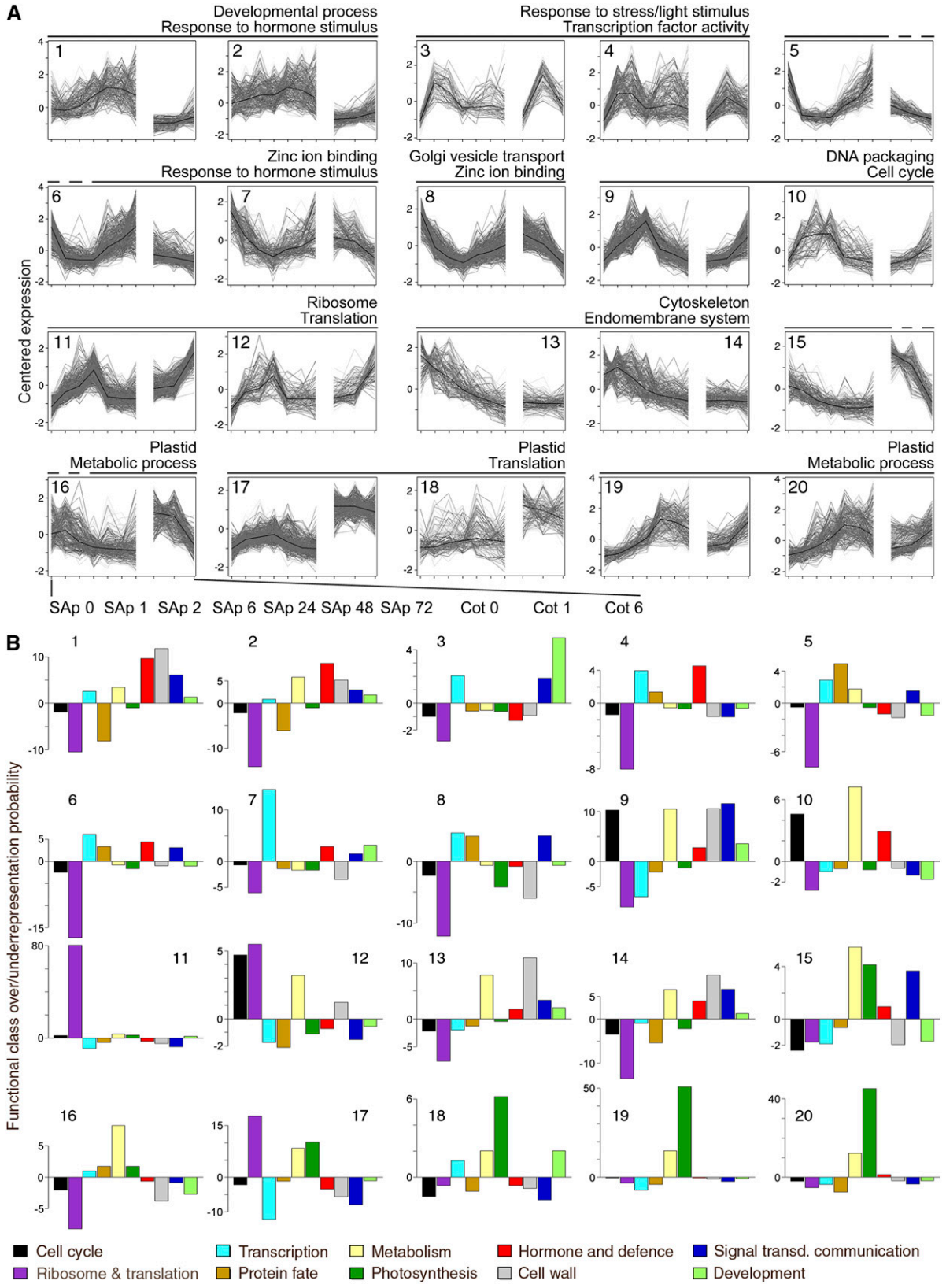

Figure 2. Unsupervised Clusters of Differentially Expressed Genes Reveal Dynamic Cellular Processes upon Deetiolation.

higher expressed in dark shoot apices than cotyledons. None of those loci has been identified through forward genetic screens or has had documented knockout phenotypes. While this highlights the possibility of genetic redundancy within this large family of proteins, it underlines the valuable role of expression profiling. Genes for RING proteins upregulated by light, predominantly in the apex (exemplified by At5g41400, for a predicted secretory protein), were rare.

Another group of proteins identified by GO term overrepresentation were the leucine-rich repeat–containing transmembrane receptor kinases (LRR-RKs), a family of signal transducers greatly expanded in plants. Some of these proteins have roles in development and defense, but for the majority of family members the roles have not been uncovered (Dievart and Clark, 2004). An interesting feature is the transient, phased induction of distinct, coregulated groups of LRR-RKs, mostly in the shoot apical region (Figure 4B). These expression patterns are consistent with the possibility that a number of these receptor kinases are involved in the development of specific cell types, partly by influencing cell wall assembly (Clay and Nelson, 2002; Eyuboglu et al., 2007).

A very large number of other protein kinases, specifically proteins in the mitogen-activated protein kinase (MAPK) cascades, were also among genes rapidly repressed by light (see Supplemental Figure 4 and Supplemental Table 5 online). The function for one MAPK kinase kinase gene, At2g30040, rapidly upregulated by light, has been tested by Quail and coworkers (Khanna et al., 2006) in gene knockout lines, but only a minor photomorphogenic phenotype was found. Interestingly, this gene shows no differential response between shoot apices and cotyledons. On the other hand, we identified several MAPK-related genes, notably At4g38470 and the stress-related At2g43790, for which high dark expression and rapid light downregulation were much more pronounced in the shoot apex. The PP2C family of protein phosphatases also included many genes rapidly downregulated by light in the shoot apex, although a group of members peaked at 6 h and another group peaked at the time of leaf primordia expansion (see Supplemental Figure 4 online).

Transcription Factor Gene Families Show Negative Light Regulation in the Shoot Apex

Transcription factors were strongly overrepresented among rapidly light-regulated genes, in clusters 3 to 8, and in supervised patterns of genes transiently upregulated (Figure 2; see Supplemental Figure 2 online). However, while we were unable to identify any transcription factor gene showing shoot apex–specific, early light induction, light triggered the downregulation of a substantial number of such genes. We monitored the basic helix-loop-helix (bHLH) and bZIP families of transcription factors (Figures 4C and 4D), because they were overrepresented among the differentially expressed transcription factor families (see Supplemental Figure 5A online), and both contain members with well-characterized roles in light responses. HY5 and HY5 homolog (HYH) are both bZIP proteins (Holm et al., 2002), while Phytochrome-Interacting Factor3 (PIF3) and PIF3-like1 both belong to the bHLH class (Monte et al., 2004). Among these two classes, genes previously identified as light-regulated responded similarly in apical and cotyledon samples, while our analysis uncovered other bZIP and bHLH transcription factor genes rapidly repressed by light specifically in shoot apices and not previously known to be light regulated (Figures 4C and 4D). These included bZIP61 and the G-box binding factor bZIP41/GBF1. Similarly, while PIF3 was more highly expressed in cotyledons, bHLH147 and bHLH121 displayed the highest levels in the apical region in the dark. A smaller number of these transcription factors, particularly of the bHLH class, were upregulated more slowly but also exclusively in the shoot apex (Figure 4C).

Two other classes of transcription factors were monitored, although they did not show the same extent of global regulation. GATA factors are zinc finger proteins that recognize GATA motifs frequently present in light-regulated promoters, particularly those of photosynthetic genes (Manfield et al., 2007). A number of MYB factors appeared among genes rapidly and transiently light-regulated in cotyledons. Among these two classes (see Supplemental Figure 6 online), rapid upregulation occurred in both shoot apices and cotyledons for Golden-like2, with a role in chloroplast biogenesis (Fitter et al., 2002), and MYB-related Circadian Clock–Associated1 and Late, Elongated Hypocotyl, central components of the circadian oscillator (Alabadi et al., 2001). MYB3R4 (At5g11510) was previously associated with cell cycle reentry (Menges et al., 2005). This gene, indeed, showed maximum expression at 6 h in shoot apices, corresponding to a group of cell cycle regulators (see below). Smaller families of transcription factors highly represented among our selected genes included the Auxin Response Factors (ARFs) and the Growth Regulatory Factors (GRFs), which are related to the phytohormones auxin and GA, respectively (see Supplemental Figures 5B and 5C online; see below).

Large-Scale Hormonal Responses Take Place during Light-Mediated Meristem and Leaf Primordia Activation

Hormone-related GO terms appeared frequently associated with our differential gene clusters and selected patterns (Table 1; see Supplemental Table 4 online). In order to systematically test the involvement of hormone-regulated pathways in the light response, we examined sets of robust hormone-regulated genes identified by a previous meta-analysis (Nemhauser et al., 2006).

Figure 2. (continued).

(A) Expression levels of genes in 20 clusters identified among the 5794 differentially expressed genes by the K-means algorithm. The *x* axis shows samples (Cot, cotyledon; SAp, shoot apical meristem) and times (h) after transfer from dark to light, as shown at the bottom of cluster 16. The *y* axis shows expression values (log2) centered around the median for each gene. Labels above one or more consecutive clusters indicate selected, overrepresented GO terms (from a complete list available in Table 1).

(B) Histograms showing the probability of overrepresentation/underrepresentation of selected functional classifications for each gene cluster.

Table 1. Selected Overrepresented GO Terms within Each of the Unsupervised Clusters of Differentially Expressed Genes, Shown in Figure 2

Cluster Number	Selected Overrepresented GO Term	P Value
1, 2	Developmental process	5.0 e-05
	Response to hormone stimulus	2.3 e-06
	Cell morphogenesis	2.7 e-04
3, 4	Response to stress	8.5 e-08
	Response to light stimulus	3.8 e-05
	Transcription factor activity	0.00083
5, 6, 7	Zinc ion binding	8.4 e-05
	Transcription factor	6.8 e-04
	Response to hormone stimulus	3.5 e-07
	MAPK	1.0 e-03
8	Golgi vesicle transport	7.1 e-04
	Zinc ion binding	0.00099
9, 10	DNA packaging	2.0 e-14
	Cell cycle	5.1 e-09
11, 12	Ribosome	1.6 e-72
	Translation	9.6 e-65
	Metabolic process	3.2 e-13
13, 14	Cytoskeleton	1.7 e-06
	Endomembrane system	6.3 e-05
15, 16	Plastid	4.3 e-07
	Metabolic process	5.3 e-04
17, 18	Plastid	4.2 e-167
	Metabolic process	5.7 e-05
	Translation	1.2 e-20
19, 20	Plastid	3.7 e-36
	Metabolic process	2.3 e-5

We only used the top upregulated or downregulated genes for each hormone, although the cutoff point varied depending on the hormone (see Methods).

Genes robustly upregulated by auxin were statistically overrepresented within the genes following supervised patterns downregulated by light in apical tissue within the first 6 h of light (Figure 5B). Such genes included the transcription factor *Arabidopsis thaliana* Homeobox2 (HAT2), and several Auxin/Indole-3-Acetic Acid and Small, Auxin-Upregulated proteins (Figure 5A). The converse was true for auxin downregulated genes, including the cell wall–related Arabinogalactan Protein13 and the LRR-RK At5g60890, which were upregulated by light early in shoot apices (Figure 5A; see Supplemental Table 5 online). Interestingly, a distinct group of auxin-induced genes became highly expressed in apical tissue after 1 to 3 d in the light, at the time of rapid development of leaf primordia. This is consistent with the waves of ARF transcription factors, several of which, including the MONOPTEROS gene (ARF5), became highly expressed at the time of primordia development (see Supplemental Figure 5B online).

Genes indicative of ethylene function exhibited somewhat similar behavior to those regulated by auxin. The highest expression value for ethylene downregulated genes was often observed in the light, particularly at 6 h after induction (Figures 5C and 5D). Again, this may indicate a rapid depletion of ethylene or inhibition of its signaling pathway by light, most notably in the apical tissue. Consistent with this notion, two genes for Aminocyclopropane Carboxylic Synthases, At4g37770 and, particularly, At4g11280, key enzymes in ethylene biosynthesis, and the important ethylene-dependent transcription factor Ethylene-Insensitive3, were rapidly, transiently downregulated by light in shoot apices. Genes regulated by another stress-related hormone, abscisic acid, were also monitored. Similar to ethylene, abscisic acid downregulated genes were more often elevated than downregulated by light, but the overall link between abscisic acid and light regulation was far less consistent (see Supplemental Figure 7 online).

Contrary to auxin- and ethylene-responsive genes, the shoot apex exhibited a positive response to cytokinin in the light (Figures 5E and 5F). Cytokinin-responsive genes were induced in waves of different expression timing, many reaching their highest expression at 6 h, when maximum expression of cell cycle genes also occurred (see below). Among these cytokinin-regulated genes, transcripts for several *Arabidopsis* Response Regulators (ARR5, ARR6, ARR7, and ARR16) were rapidly elevated in the shoot apex.

Only a small number of genes that can be considered robust indicators of the GA response following the selection procedure of Nemhauser and coworkers (2006) could be identified. Therefore, we present data for genes involved in the critical steps in GA metabolism and signaling. GAs are synthesized in plant cells as inactive forms, and the final conversion to generate active GA (GA_4 in *Arabidopsis*) is catalyzed by the GA 3-β-hydroxylase family (GA3ox). The most highly expressed GA3ox genes were both rapidly induced by light in shoot apical tissue, reaching a peak of expression at 2 h (Figure 5G). The previous step in GA biosynthesis is catalyzed by the products of GA20ox genes. One GA20ox gene, At5g51810, became highly expressed after 24 h, at the time of primordia expansion. The inactivation of such 3-β-hydroxylated GAs is performed by GA2ox proteins. These proteins are also induced by GAs, as a homeostatic mechanism. Two GA2ox genes were also rapidly induced by light in shoot apices. Consistent with this apparent early peak of GA action in the shoot apex in the light, the gene for the growth-repressive DELLA protein GA-Insensitive, the primary target of GA function, was highly expressed in the dark and very rapidly repressed by light in the apex (Figure 5G). Together, these observations are consistent with a model for an early, positive role of GAs in leaf initiation by light.

Brassinosteroid hormones have been shown to play an essential role during skotomorphogenesis, and their loss is sufficient to trigger a photomorphogenic-like phenotype (Li et al., 1996). We uncovered only limited transcriptome-based evidence for a consistent regulation of brassinolide-dependent genes by light (see Supplemental Figure 7 and Supplemental Table 5 online). We found that both genes upregulated and downregulated by brassinosteroids were expressed at the time of leaf primordia expansion. However, we did observe that several brassinolide downregulated genes were also downregulated by light early and specifically in apical tissue. Similarly, two negative regulators of brassinosteroid levels (*phyB* Activation-tagged Suppressor1) or signaling (Brassinosteroid-Insenstive2) were rapidly downregulated by light, while transcription factors (BRI1-EMS Suppressor1 and Brassinazole-Resistant1) that

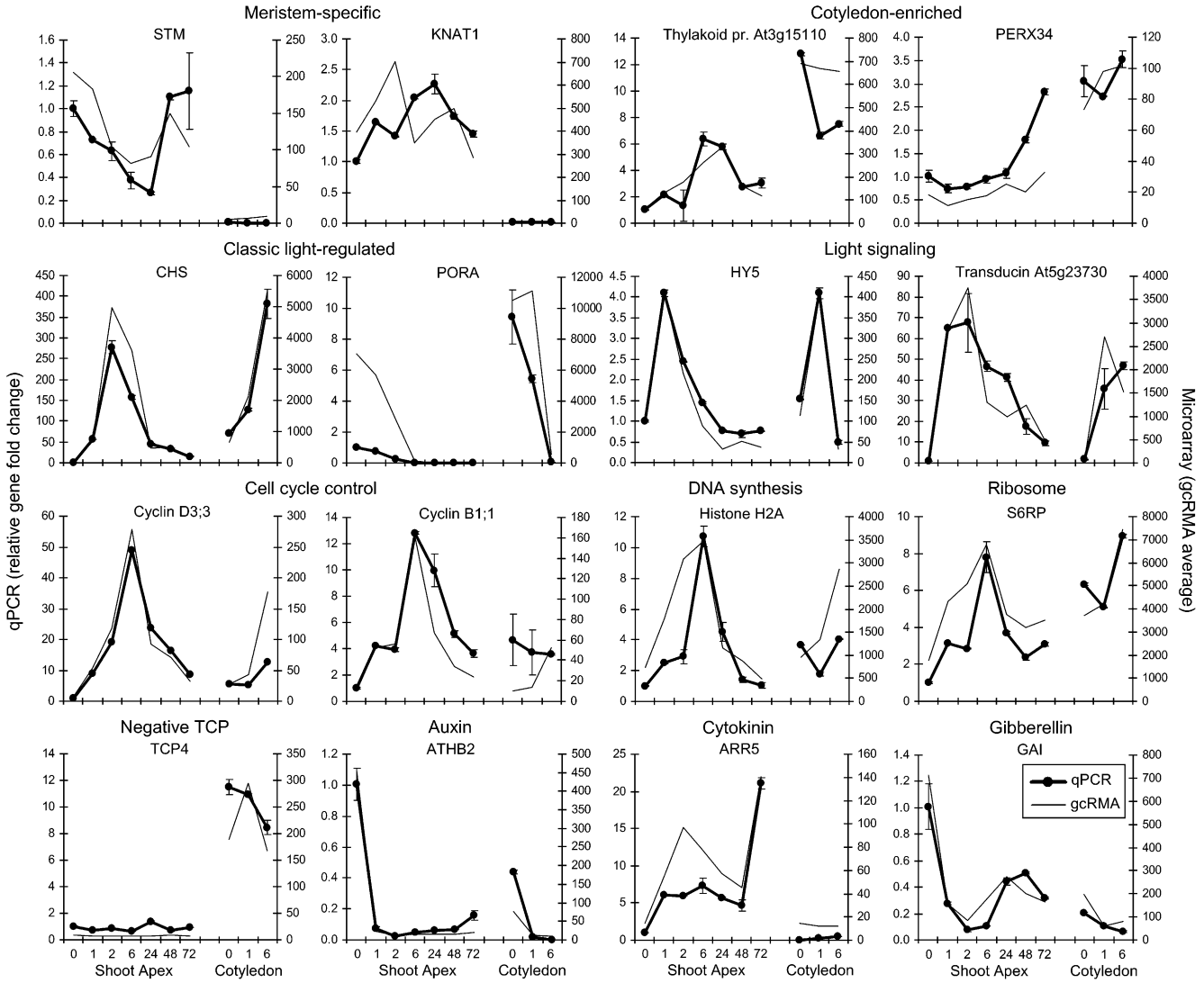

Figure 3. Validation by qPCR of Microarray-Detected Changes and of the Discrete Nature of the Samples.

Single RNA samples from the tissues and time points employed for microarray analysis were used in triplicate for relative (as a ratio against the constitutive gene *ACT2*) qPCR, using primers specific for the genes indicated. The genes were selected as representative of the processes shown above each graph. The black lines represent the expression levels from qPCR, and the gray lines represent the expression levels from gcRMA-normalized microarray values.

actively mediate brassinosteroid responses were among the genes upregulated during leaf primordia expansion. These results suggest an early and positive action of brassinosteroids in the shoot apical tissue in the light, unexpected given the genetic evidence for an active role of these hormones during skotomorphogenesis.

Cell Wall– and Turgor-Related Processes Are Light Regulated

The strength of the plant cell wall is strongly regulated during growth (Cosgrove, 2005). Therefore, we monitored genes encoding proteins involved in cell wall loosening. A substantial number of genes of the xyloglucan endotransglycosylase family and expansins showed very pronounced expression coinciding with the later phase of rapid cell division and the initial expansion of leaf primordia. Several cellulose synthase family genes (e.g., At1g02730; see Supplemental Table 5 online) also showed a rapid upregulation in shoot apical tissue. Cell expansion takes place through a combination of cell wall modification and internal turgor pressure, and significantly, a large number of aquaporins exhibited very high expression in developing leaf primordia (see Supplemental Figure 8 online). Genes showing this pattern of expression included primarily those encoding proteins localized to the plasma membrane (like Plasma membrane Intrinsic

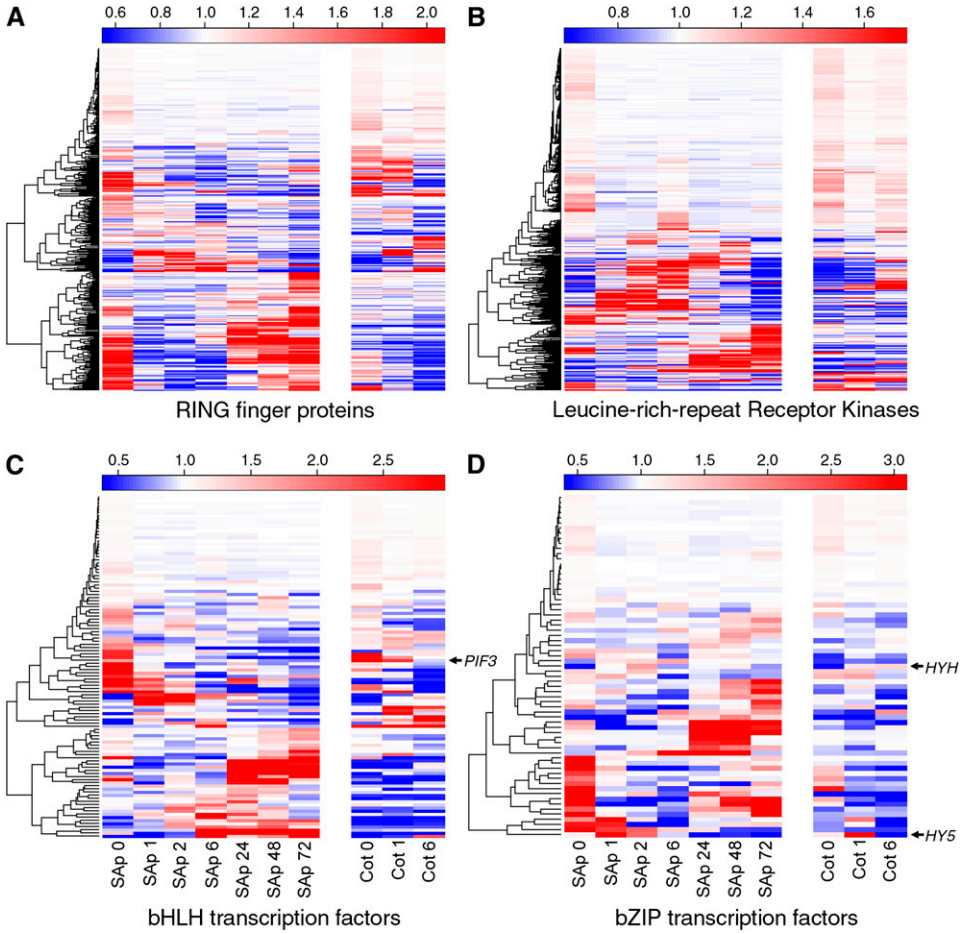

Figure 4. Heat Maps of Expression Levels of Genes Encoding Proteins Involved in Signaling.

RING proteins **(A)**, LRR-RKs **(B)**, and transcription factors of the bHLH **(C)** and bZIP **(D)** classes were analyzed. The scale of expression (linear values, ratio to mean across samples) is shown above each heat map. The samples and time points (as for Figure 3) are listed at the bottom of **(C)** and **(D)**. Genes are arranged (*y* axis) according to the similarity of expression (hierarchical clustering). These gene families included numerous members regulated by light specifically in shoot apices. Cot, cotyledon; SAp, shoot apical meristem.

Protein14 [PIP14]/At4g00430 or PIP26/At2g39010) but also some located to the tonoplast (Tonoplast Integral Protein/At2g36830).

Light Stimulates a Coordinated Increase in the Expression of Cell Cycle and Protein Synthesis Genes

Two of the more consistently regulated groups of genes identified by unsupervised clustering were highly enriched in genes associated with the cell cycle or DNA packaging (clusters 9 and 10) and those related to ribosome or translation (clusters 11 and 12) (Figure 2). Their main peak of expression occurred at 6 h in both shoot apices and cotyledons; however, genes in the clusters containing ribosome constituents were expressed at substantially higher levels in cotyledons. Given the importance of these two processes, we examined the behavior of core cell cycle genes and of ribosomal and translation genes.

In the dark, typically, the ribosomal protein genes were expressed at substantially lower levels in shoot apices than in cotyledon samples. Rapid upregulation by light took place in the shoot apex, with maximal expression in both tissues at 6 h. At 24 h, when cell division remains active but becomes restricted to the developing leaf primordia (Figure 6; see below), expression in shoot apices returned to the same levels encountered in darkness. We monitored other genes involved in protein translation from the Factors in *Arabidopsis* Translation database (http://research.cm.utexas.edu/kbrowning/fiat/). Among these genes, likely to include positive and negative regulatory factors, one identified group correlated positively with the pattern of ribosomal protein expression, while a second, small group displayed the inverse pattern (Figure 6). The TCP family of transcription factors includes members that play a role in the transcriptional regulation of ribosome biogenesis (Li et al., 2005; Tatematsu et al., 2005). Apart from cyclin B1;1 (At4g37490), a mitotic cyclin with TCP homology, one TCP factor (At2g45680) was upregulated by light specifically in the shoot apex (Figure 6) ahead of the ribosomal 6-h maximum. Interestingly, class II TCPs have a proliferation-inhibitory function, and several such

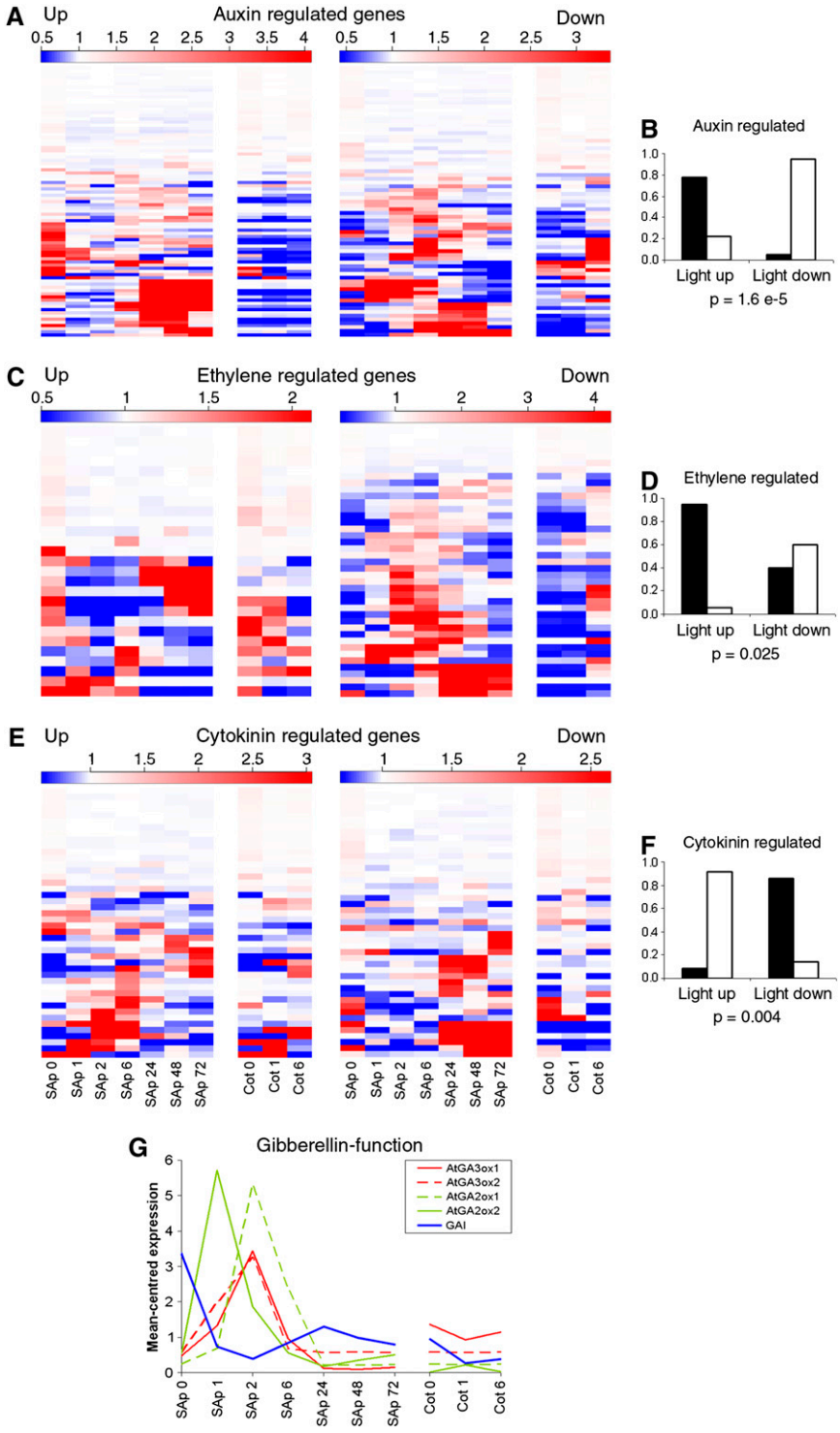

Figure 5. Expression Profiling Indicates Hormone Actions in the Shoot Apex upon Transition to Light.

(A), **(C)**, and **(E)** Pairs of heat maps of expression levels of genes previously identified as robustly upregulated or downregulated by auxin **(A)**, ethylene **(C)**, and cytokinin **(E)**.

(B), **(D)**, and **(F)** Histograms showing the proportion of genes downregulated (black bars) or upregulated (white bars) by auxin **(B)**, ethylene **(D),** and cytokinin **(F)** and present in the groups of supervised patterns representing upregulation or downregulation by light in shoot apical tissue. The P values from a test for lack of association between the hormone and the light response are also indicated.

(G) Expression of key genes in the biosynthesis (red traces) or catabolism (green traces) of active GA, or a target and negative regulator of GA action (blue trace), all of which suggest a rapid, positive regulation of GA responses by light in shoot apices. Cot, cotyledon; SAp, shoot apical meristem.

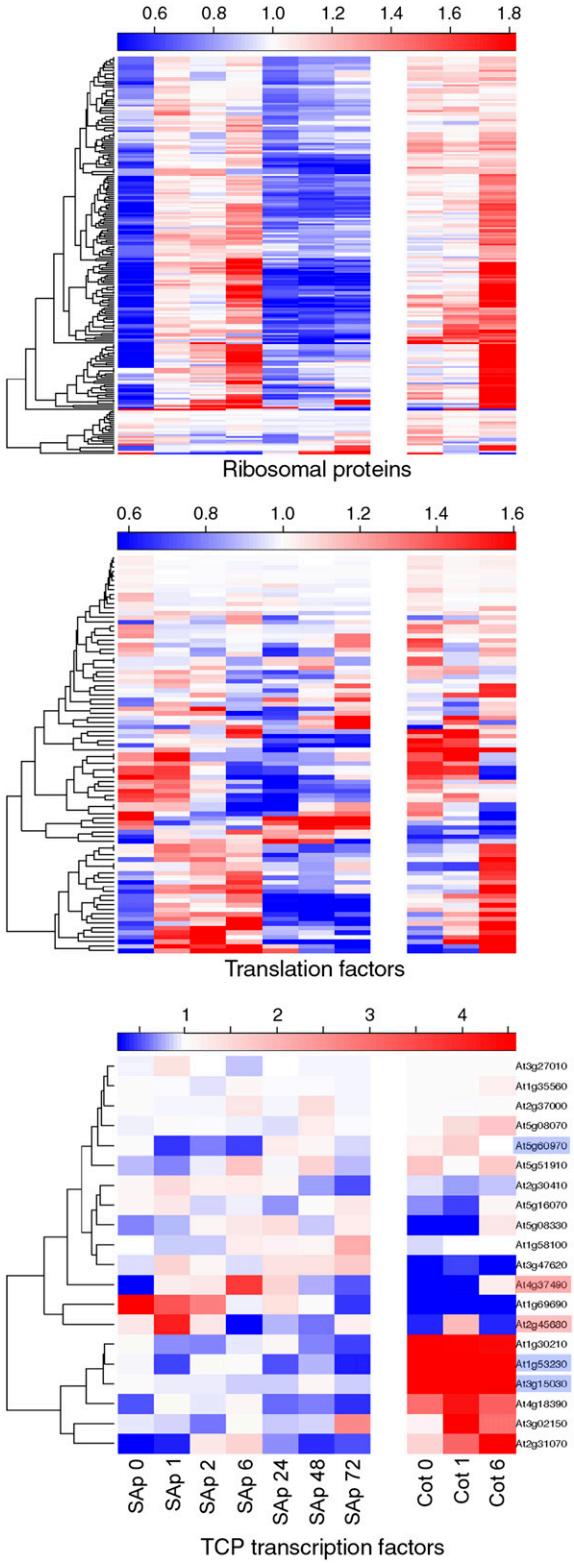

Figure 6. Heat Maps of Expression Levels of Genes Encoding Ribosomal Proteins (Indicating a Strong, Coordinated Cell Growth Induction by Light in Shoot Apices and, to a Lesser Extent, Cotyledons), Other Genes Involved in Translation, and Transcription Factors of the TCP Family.

Individual rectangles highlighting the accession numbers indicate positive (red) or negative (blue) TCP transcription factors referred to in the text. Cot, cotyledon; SAp, shoot apical meristem.

genes exhibited cotyledon-specific expression (At1g53230 and At3g15030), while one showed downregulation of expression by light in shoot apices (At5g60970) (Figure 6).

The circadian clock controls the expression of at least 15% of the genome, and many clock-dependent genes are also light regulated (Harmer et al., 2000; Edwards et al., 2006). Indeed, one-third of genes identified as differentially expressed in our study (1926 of 5794 genes; see Supplemental Table 5 online) had been identified as genes with circadian behavior by Edwards et al. (2006). For example, changes specific to the 6-h time point relative to 0, 24, 48, and 72 h could well fit a circadian regulation. This pattern is close to that characteristic for ribosomal genes, but only 4 of 189 ribosome-related genes had been shown to be rhythmic. Circadian regulation, therefore, does not explain the coordinated expression we observed at 6 h.

We monitored the expression of core cell cycle genes (Vandepoele et al., 2002), the values for all of which are given in Supplemental Table 5 online. We supplemented these with genes associated with mitosis and DNA synthesis (Menges et al., 2005). Six groups of genes were identified computationally (see Methods), which we arranged according to the timing of their expression (Figure 7B). Groups 1 and 2 were those highest expressed in dark-grown shoot apices, with group 1 declining rapidly. A cyclin-dependent kinase (CDK) inhibitor, Kip-Related Protein4 (KRP4), and CKL3, a member of a family of CDK-like genes of unknown function, were particularly rapidly repressed by light. CKL3 was previously linked to G1/S-phase control (Menges et al., 2005). Groups 3 to 5 represent distinct expression timings, although the boundaries between different groups were not sharp. Group 3 consisted of genes rapidly light upregulated and included genes expressed early in G1. Group 4 included a probe set representing both CDKB1;1 and CDKB1;2 as well as cyclinA2;3 (CYCA2;3). Group 5 had the largest number of genes, all peaking in expression at 6 h. These included genes acting in both the G2/M transition, like CYCB1;1, and the G1/S transition, like CYCD3;3, raising the possibility that cells had remained arrested in the dark at both transition points. Consistently, genes associated with both DNA synthesis (like histones) and mitosis (like the syntaxin KNOLLE) were part of group 4 or 5. Expression changes in group 6 and partly in group 5 are consistent with a return to G1-phase. Such genes included both components of the anaphase-promoting complex (APC) and CYCD3;1.

We sought further evidence for the co-occurrence of cells undergoing mitosis and those in S-phase in the shoot apical region by monitoring genes associated in expression with both processes (Menges et al., 2005), and including as S-phase indicators histones (http://www.chromadb.org) and origin recognition complex genes (Masuda et al., 2004). Indeed, the timing of both groups of genes largely coincided, but, as expected, mitosis genes were often more highly expressed in shoot apices, while S-phase–associated genes were also abundant in cotyledons undergoing endoreduplication (see Supplemental Figure 9 online).

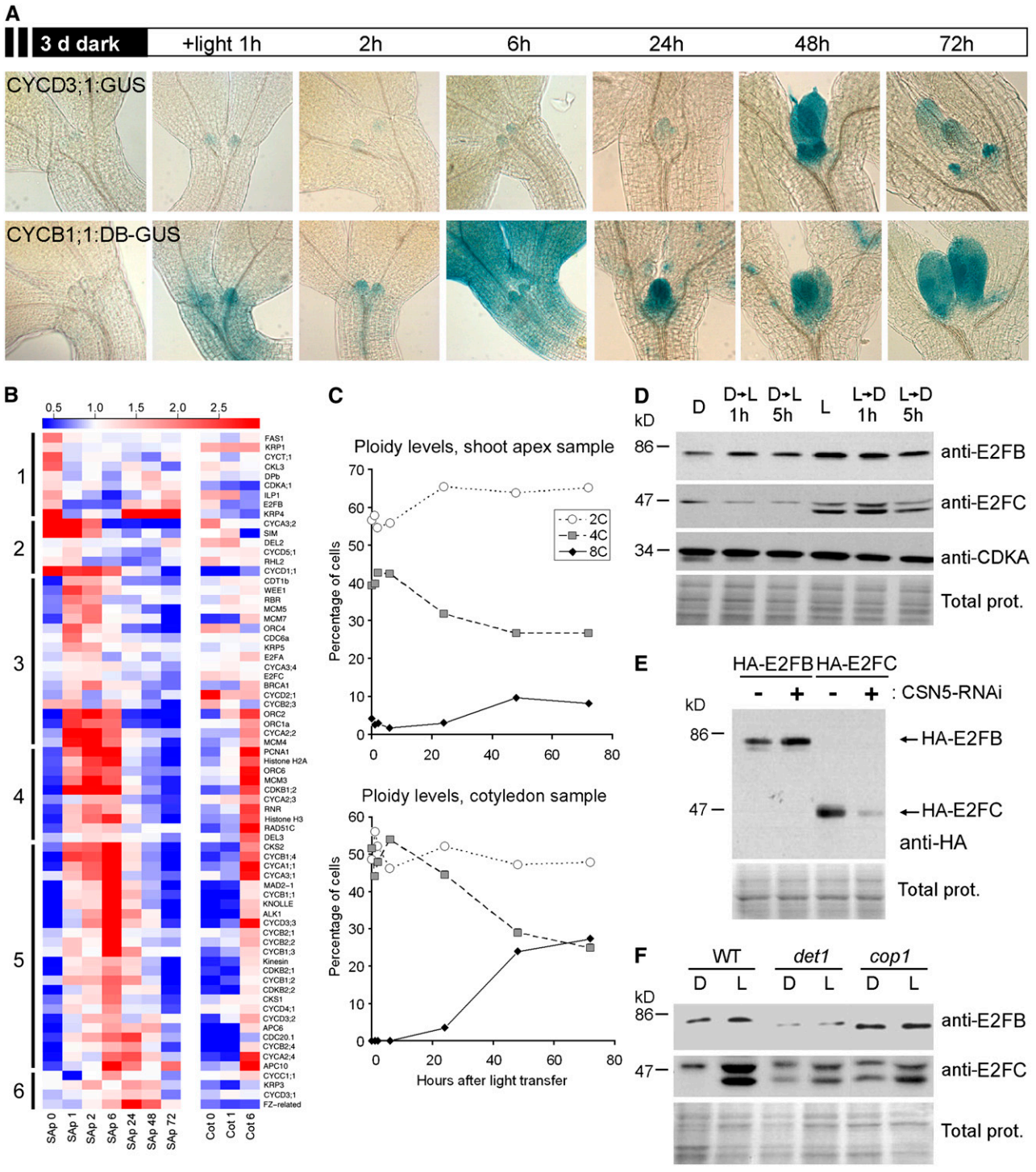

Figure 7. Light Control of Cell Cycle Activity.

(A) Expression of cell cycle regulators is synchronously reactivated in the shoot apex when dark-grown seedlings are transferred to light. Seedlings grown on solid medium, in the absence of sugar, were monitored for the expression of CYCD3;1:GUS, reporting an active cell cycle state, and CYCB1;1:DB-GUS, which is active during late G2 and mitosis, as indicated at various times (shown at top) following the transfer to white light.

(B) Heat map of expression levels of core cell cycle genes showing differential expression as well as genes representative of DNA synthesis, mitosis, and gap phases. Groups of genes identified by self-organizing maps are shown. Groups 1 and 2 are rapidly downregulated in shoot apices. Group 3 includes genes expressed early in G1. Groups 4 and 5 contain genes acting in both the G2/mitosis and G1/DNA synthesis transitions. Group 6, and partly 5, indicates a return to G1.

Light Rapidly Stimulates the Expression of Cyclins in the Apical Region

We exploited β-glucuronidase (GUS) reporter constructs to visualize the extent of cell cycle activity of dark-grown seedlings transferred to light. Two constructs were monitored. CYCD3;1:GUS, a regulator of the G1/S transition (Dewitte et al., 2003), and CYCB1;1:DB-GUS, which reports a mitotic cyclin expressed from late G2 until anaphase (Colon-Carmona et al., 1999). Seedlings grown for 3 d in the dark without sucrose had undetectable levels of CYCB1;1 or CYCD3;1 expression (Figure 7A). Following transfer to light, while no clear changes in CYCD3;1 could be seen in the first 24 h, a rapid and very pronounced increase in CYCB1;1 promoter activity could be seen, with a peak of GUS at 6 h after light exposure (Figure 7A). Interestingly, the GUS staining at the 1- and 6-h time points was somewhat diffuse and also apparent at the base of the cotyledon and the top of the hypocotyl hook, raising the possibility that the mitosis-specific degradation of CYCB1;1 might not have taken place fully at these early time points after light exposure. In agreement, genes coding for components of APC, such as APC6 and APC10, are expressed slightly later than the majority of mitotic cyclins. The activation of these APC components could explain the disappearance of CYCB1;1:DB-GUS from the primordia between 6 and 24 h.

Apical Regions and Cotyledons Show Very Different Patterns of Cell Cycle Activity

To measure the cell cycle progression directly, we quantified the genomic DNA content per nucleus of both shoot apical and cotyledon regions by flow cytometry (Figure 7C; see Supplemental Figure 10 online). Cells in the cotyledons and the shoot apex from dark-grown seedlings had a close to equal proportion of 2C and 4C nuclei. Consistent with the finding of the rapid induction of cell cycle genes, the transition to light led to a rapid increase in the proportion of 2C nuclei at the expense of 4C in the shoot apical sample, indicating a net excess of mitosis over S-phase activity between 6 and 24 h, so that a 2C/4C distribution characteristic for proliferating tissue was apparent (Beemster et al., 2005). By contrast, in the cotyledon samples, the population of 8C nuclei increased at the expense of 4C, indicative of endoreduplication, at a later time point. The appearance of 8C nuclei in the shoot apical material (~10%) after 24 h is probably indicative of the small amount of hypocotyl hook present in the sample, as endoreduplication takes place in differentiating leaf cells but not until much later in development (Beemster et al., 2005), while the hypocotyl has much endoreduplication in the dark (Gendreau et al., 1998). Consistent with the transcription profiling, these data show that cells in dark-grown shoot apices and cotyledons are arrested with both 2C and 4C DNA content, and both groups actively reengage in cell cycling on transfer to light, primarily mitotic cycles in the case of the meristems and/or leaf primordia and endocycling in cotyledons.

Light Signaling Modulates the Amount of the E2FB and E2FC Transcription Factors, in a Process That Involves COP1 and CSN5

The observed coordinated regulation of cell cycle–related genes raised the possibility of light affecting the levels or activity of the E2F transcription factor family, transcriptional regulators playing an important role in the entry into cell proliferation or differentiation. We asked whether light signaling pathways could act on these transcription factors not only indirectly, through the activity of CDKs, but also directly, by regulating their protein levels. Protein extracts from complete dark- or light-grown seedlings were subjected to immunoblot analysis using antibodies against E2FB and E2FC. Extracts from 5-d-old seedlings grown in continuous light showed increased (2.5-fold) levels of E2FB relative to dark-grown seedlings (Figure 7D). Transfer experiments showed that an increase in E2FB levels could be detected within 1 h of light exposure. Antibodies against E2FC recognized two different protein forms, a high-mobility one being specific to light-grown seedlings. Transfer from dark to light resulted in a rapid decrease in the level of the E2FC slow-mobility form. Given the existing evidence for the regulation of protein stability as a central mechanism of light signaling, we tested the possible involvement of the CSN. We tested specifically CSN5, because this subunit is essential for the integrity of the signalosome but can also play roles individually (Wei and Deng, 2003).

Figure 7. (continued).

(C) Transfer from dark to light causes mitosis soon after the transfer in shoot apical regions (SAp), while cotyledons (Cot) exhibit endoreduplication later. Ploidy levels of shoot apices (top) or cotyledons devoid of shoot apices and cotyledon tips (bottom) were assessed by flow cytometry of 4′,6-diamidino-2-phenylindole–stained nuclei. 2C, diploid DNA quantity in G1; 4C, DNA quantity in G2. Results are from one representative experiment. Note that mitosis (4C → 2C) takes place between 6 and 24 h in the shoot meristem region, while endoreduplication (4C → 8C) takes place in cotyledons between 24 and 48 h.

(D) to **(F)** Light signaling, COP1, and the CSN5 modulate the stability and postranslational modification of E2FB and E2FC transcription factors.

(D) Immunoblot analysis of extracts from wild-type seedlings grown for 5 d in darkness (D) or continuous white light (L) or subjected to reciprocal transfers. The antibodies used in each case are shown at right, and the positions of molecular mass markers are shown at left. Total Amido black–stained protein is shown on the same membrane as a loading control.

(E) Immunoblots of extracts from *Arabidopsis* protoplasts derived from cell suspensions transformed transiently with HA-tagged versions of E2FB or E2FC or either E2FB or E2FC cotransformed (where indicated at top) with an RNAi construct for CSN5. Proteins were detected with HA-specific antibodies.

(F) Immunoblot analysis of total protein from 7-d-old seedlings of *Arabidopsis* wild type, *det1-1*, or *cop1-4*, grown in darkness or continuous white light, and challenged with the primary antibodies shown at right.

Transformation of an RNA interference (RNAi) construct of CSN5 (mutants in subunits of the CSN are lethal) into dark-grown *Arabidopsis* protoplasts (Magyar et al., 2005), together with hemagglutinin (HA)-tagged versions of E2Fs, showed an increase in E2FB level and a decrease in E2FC (Figure 7E). No high-mobility form of E2FC was present in protoplasts.

The role of DET1 and COP1 was tested using mutants *det1-1* and *cop1-4*. Seven-day-old seedlings were used in these experiments to ensure complete development of mutant seedlings (Figure 7F). While in the wild type, E2FB levels were induced by light, in *cop1*, E2FB protein levels were constitutively elevated, independent of light. Similarly, no light regulation of E2FB was apparent in *det1*, but the level of E2FB was reduced. The two forms of E2FC in light-grown wild-type seedlings were constitutively present in both *det1* and *cop1*.

Among the three E2F proteins, putative target genes for E2FA have been experimentally determined by profiling the transcriptional influence of the overexpression of E2FA and its dimerization partner, DPa (Vandepoele et al., 2005). We monitored the overlap between our gene set and genes whose expression was altered in 35S:E2FA plants. Genes identified as positively regulated by E2FA, including many DNA synthesis–related factors, were frequently positively regulated by light, coinciding with the maximal cell cycle activity at 6 h (see Supplemental Figure 11 online). Genes repressed in plants with elevated levels of E2FA included a substantial number of metabolic enzymes and plastid proteins and displayed varied responses to light, from early repression to late induction, in consecutive waves comparable to those of the LRR-RKs (see Supplemental Figures 11 and 12 and Supplemental Table 5 online).

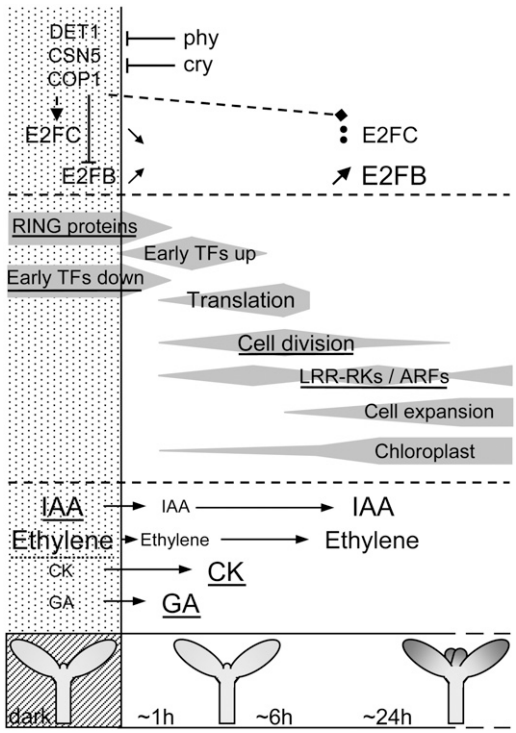

Figure 8. Model Time Sequence Taking Place in the Shoot Apex upon Deetiolation.

Top, changes in protein levels. Arrows represent promotion, blocked arrows represent repression, and the diamond-tipped arrow represents another effect (the appearance of multiple protein forms). The oblique arrows associated with E2FC and E2FB, and relative font sizes, represent increases or decreases in protein level upon transfer to light, and the two dots next to E2FC represent two forms of differential mobility. In the dark, the activity of DET1, COP1, and CSN5 causes reduced levels of E2FB and elevated levels of E2FC. These activities are repressed by the action of phytochrome and cryptochrome photoreceptors. Middle, changes in mRNA expression. The width of the gray bar is representative of expression levels. Bottom, changes in the expression of genes associated with hormone action, represented by the font size of the hormone name. Processes for which cotyledons show no or very reduced response are underlined. The dark shading at left represents darkness. An approximate time scale, after transfer to light, is indicated at bottom.

DISCUSSION

Timeline of Light Responses in Shoot Apices and Cotyledons

Plant development is intimately connected to environmental signals, so studies of environmental responses have the potential to provide unique insights into developmental programs. We have undertaken a genome-wide expression analysis upon light activation of seedling shoot apices and cotyledons, and this enabled us to identify the associated sequence of events, many of which had remained masked in the analysis of whole seedlings (Figure 8). In the shoot apex, light triggered the rapid down-regulation of expression for specific transcription factors and genes in ubiquitination pathways. This suggests the loss of repressors that had been active in the dark. Light also initiated rapid hormonal responses in the shoot apex: the transient repression of auxin and ethylene action and the activation of cytokinin and GA action. The initial rapid gene expression changes were followed by a coordinated increase in translation-associated genes and subsequently by cell cycle genes involved at both the G1- to S-phase and G2 to mitosis transitions. After the waves of translation and cell cycle activity, transcript changes indicate that the initial leaf primordia expansion is driven or accompanied by cell wall modification and the generation of turgor pressure (24 to 72 h). At this time, a specific group of auxin-regulated genes also increase in expression, as do other differentiation processes, such as the photosynthetic buildup. Only some of these light responses are common to both shoot apices and cotyledons, including some of the positive transcriptional responses, the increase of translation-associated genes, the induction of a subset of chloroplast biogenesis genes, and the induction of cell cycle genes, although in the case of cotyledon this relates to an altered cell cycle program, endoreduplication. The DET and COP complexes are central repressors of photomorphogenesis, being active in the dark. They mediate, in a coordinated fashion, the opposite regulation of E2FB and E2FC protein levels by light. This raises the possibility that the balance

of these transcription factors is central to the light-induced gene expression program.

Early Light Responses Specific to the Shoot Apex Involve the Rapid Repression of Genes Coding for RING Finger Proteins and for Distinct Classes of Transcription Factors

Targeted degradation of repressors has emerged as a central theme both in light signaling and in phytohormone responses. Although the primary regulation of signal-dependent proteolysis is at the levels of activity and localization of E3 ubiquitin ligases, our study shows that these are corroborated by their regulated transcription. For instance, RING finger proteins are implicated in signal-dependent protein degradation and in the modification and broad activation of chromatin (Fleury et al., 2007). We found that large numbers of genes coding for RING finger proteins were rapidly downregulated specifically in the shoot apices. While this was the case for the majority of genes coding for RING finger proteins, SPA1, which is an established coactivator of COP1, was rapidly light-induced. SPA1 might function to associate with and maintain RING finger proteins such as COP1 out of the nucleus in the light (Hoecker et al., 1999; Yang and Wang, 2006). Targets of RING finger protein–mediated degradation include transcription factors such as HY5, whose protein stabilities are promoted by light (Osterlund et al., 2000). We found that this is also corroborated by the induced expression of HY5 upon light exposure (Figures 3 and 4).

Previous time-resolved studies of light responses in whole seedlings have highlighted the role of early induced transcription factors (Tepperman et al., 2001, 2006; Monte et al., 2004). Contrary to this, in the shoot apex a large number of transcription factors showed a negative regulation by light, including members of the bZIP and bHLH families. Loss of the G-box binding factor GBF1 among these has been identified as causing an exacerbated but complex response to blue light (Mallappa et al., 2006), while for the others no functional information exists.

Hormone Responses in the Light Activation of Meristem Activity and Leaf Initiation

A large body of experimental work has examined the involvement of phytohormones in the responses of plants to light, but the results have often been difficult to interpret due to tissue-specific responses (Nemhauser, 2008).

Auxin is thought to be high in the apex, with auxin maxima at the sites of leaf primordia initiation and in the central meristematic dome (de Reuille et al., 2006). Our data revealed that a large cohort of auxin-responsive genes, including HAT2, are highly expressed in the shoot apex in the dark and rapidly downregulated by light. This is somewhat unexpected and suggests that increased auxin concentration and/or responsiveness could be part of the repressive mechanism of meristem function in the dark. A state of high auxin action in elongating organs is also known to occur in the dark or in response to shade signals. During shade avoidance, which involves internode elongation at the expense of leaf lamina growth, a strong auxin response is initiated by a decrease in active phytochrome (Devlin et al., 2003). Two auxin-responsive transcription factors, HAT2 and HAT4, were found to be highly induced by such phytochrome-inactivating shade signals (Devlin et al., 2003). Conversely, HAT4 was identified as an early red light–repressed gene in etiolated seedlings (Tepperman et al., 2004).

We found the expression of the gene for the PIN1 auxin transporter to be transiently upregulated by light in the shoot apex. Although PIN1 physiological activity is mostly determined through its localization, it is possible that the increased PIN1 level might contribute to direct the auxin flow away from the meristem upon light exposure. Light might also act to downregulate auxin responsiveness, since HY5 and HYH, two key bZIP transcription factors functioning in the light, also act as negative regulators of auxin responses (Sibout et al., 2006). Consistent with the role of auxin in the light-mediated deetiolation of the shoot apex, it has been observed that loss of a calossin-related protein, BIG, involved in auxin transport, causes deregulated expression of light-responsive genes in the dark (Gil et al., 2001), and gain-of-function mutation of Suppressor of *hy2*/Indole-3-Acetic Acid3, a repressor of auxin responses, can lead to a small degree of leaf development in the dark (Tian et al., 2002).

A distinct cohort of auxin upregulated genes increased in expression at a later time point, coinciding with leaf primordia development. Therefore, we could distinguish two stages of the auxin response to light: a drop in the shoot apex between 0 and 6 h that accompanied entry into the cell cycle, and an elevation between 6 and 24 h, which accompanied the beginning of leaf primordia expansion and differentiation. Context-specific roles for auxin are thought to occur through the expression of specific auxin response transcription factors (ARFs) (Kepinski, 2006). Interestingly, light triggered waves of expression of distinct ARFs in the shoot apex (see Supplemental Figure 5 online). ARF3 and ARF4 show maximal induction exclusively in the apex at 6 h, preceding leaf primordia expansion, and have been found to play essential roles in leaf morphogenesis (Pekker et al., 2005).

Expression of ethylene-responsive genes followed a similar trend to those of auxin, high in the dark and during leaf primordia expansion. The parallel auxin and ethylene responses might be explained by the finding that auxin biosynthesis is under the control of ethylene (Swarup et al., 2007). Ethylene was also found to determine the balance between the proliferation and quiescence of stem cells in the root and was proposed as a potential mediator to couple environmental signals to plant growth (Ortega-Martinez et al., 2007). Ethylene is in most cases associated with decreased cell expansion, but this is not always the case. In fact, phytochrome-defective pea (*Pisum sativum*) plants have exaggerated elongation of internodes, yet they accumulate elevated levels of ethylene and their phenotypes can be rescued by ethylene biosynthesis inhibition (Foo et al., 2006).

The coordinated expression of auxin-responsive genes in dark-grown shoot apices thus could be a combined result of (1) increased auxin levels resulting from ethylene biosynthesis, (2) auxin accumulation in the apex due to low expression of auxin transporters, and (3) increased auxin response due to the instability of HY5 and HYH.

Contrary to auxin and ethylene, cytokinin- and GA-responsive genes were activated by light, with distinct kinetics. The action of cytokinin, the classical cell division–promotive hormone, has

emerged as central to the function of the shoot apical meristem (Shani et al., 2006). For example, the loss of activity of cytokinin receptors causes premature termination of shoot meristem function (Higuchi et al., 2004). Furthermore, cell proliferation in the meristem periphery is promoted by KNAT1 via cytokinins (Jasinski et al., 2005) while being kept outside the stem cell niche proper, by the action of Wuschel and A-type ARRs, which repress cytokinin responses in the center (Leibfried et al., 2005). While no regulation of cytokinin levels during deetiolation could be measured in whole seedlings, exogenous cytokinin application to etiolated seedlings mimics photomorphogenesis (Chory et al., 1994).

A rapid light induction of genes coding for GA biosynthesis and catabolism enzymes suggests an early, transient rise in GA levels upon illumination, specifically in the shoot apex. Light is well known to activate GA biosynthesis genes during the control of germination (Yamaguchi et al., 1998). The GA rise is concurrent with a drop in the expression in the shoot apices of GA-Insensitive, a transcriptional repressor of GA-dependent responses. It is known that GAs promote leaf expansion at the expense of meristem maintenance (Hay et al., 2002). Indeed, those authors observed that the expression of GA biosynthetic genes is kept precisely outside the meristem by the combined action of KNAT1 and STM. Thus, a high-CK, low-GA regime is required for the maintenance of the stem cell niche (Jasinski et al., 2005). In the light of this finding, our observed parallel increase in both CK and GA responses in the shoot apex seems paradoxical, as is the fact that *KNAT1* expression increases somewhat in parallel with GA biosynthesis genes (Figure 2). However, in our experiment, we could not resolve the spatial distribution of gene expression within the shoot apex, including the meristem (the KNAT1 and STM expression domain), and in the incipient leaf primordia, where GA biosynthesis takes place (Hay et al., 2002).

Activation of Protein Translation and Cell Proliferation during Plant Growth

Genome-wide gene expression studies have helped to unravel growth-related physiological and developmental gene-regulatory programs, such as the activation of axillary buds upon decapitation (Tatematsu et al., 2005), the synchronous induction of lateral roots from the root pericycle by auxin (Vanneste et al., 2005), seed germination (Masubelele et al., 2005), leaf development (Beemster et al., 2005), and the synchronous proliferation of cells in culture (Menges et al., 2005). These studies have established a coordinated regulation for a number of genes involved in growth and cell proliferation (Beemster et al., 2005). A total of 42% of the lateral root initiation genes, and 48% of genes upregulated or downregulated during axillary bud outgrowth, were also differentially expressed in our study, including the induction of large numbers of ribosomal protein and cell cycle genes. Tatematsu and collaborators (2005) identified promoter elements present in the majority of upregulated bud genes, particularly those of ribosomal proteins, as being similar to elements bound by transcription factors of the TCP class (Tremousaygue et al., 2003). TCP transcription factors are responsible for growth responses associated with branching architecture or petal morphology and are classified into growth-promotive (class I) and growth-inhibitory (class II) classes (Aguilar-Martinez et al., 2007). We found that the class II TCP3, TCP4, and TCP24 were constitutively expressed only in cotyledons, consistent with the expression of TCP3 in young embryo cotyledons (Koyama et al., 2007). Our data show that TCP5 is expressed at high levels in the dark and becomes downregulated by light specifically in the shoot apex, thus being a candidate repressor of meristem reactivation. Meanwhile, at least one class I TCP factor was upregulated by light specifically in the shoot apex, ahead of the expression of ribosomal genes.

The cell (cytoplasmic) growth–associated genes showed highest expression at 6 h among our samples and had returned to dark levels at 24 h, while genes positively implicated in cell cycle progression, such as A-, B-, and D-type cyclins and CDKBs, were induced less rapidly and had not returned to basal levels by 24 h, suggesting that a burst of protein translation preceded the proliferation response. This order of events indicates that, as in yeast (Neufeld and Edgar, 1998), cytoplasmic cell growth can be placed upstream of cell division also in plant meristems.

Interesting parallels can be drawn by comparing the activation of cell division of the root meristem that drives germination (Masubelele et al., 2005), the induction of pericycle cell division that drives lateral root initiation (Vanneste et al., 2005), and the light activation of meristem development in our data. In all cases, the earliest event is the rapid repression of specific CDK inhibitors. These inhibitors are KRP1 and KRP2 in the pericycle (Vanneste et al., 2005) and KRP4 in the root and shoot meristems (Masubelele et al., 2005; our data). In roots of dormant seeds as well as in the pericycle in the root, cells are arrested in G1. During germination, G1 regulators are induced first at 12 h, and this is followed by a peak of mitotic regulators at ~36 to 42 h (Masubelele et al., 2005). By contrast, we find that cells in the shoot apex are arrested both at G1- and G2-phases in the dark; in the light, B-type CDKs (CDKB1;1 and CDKB1;2) and some A-type cyclins (CYCA2;2) are induced rapidly (within 1 h), this being followed by the induction of a group of D-, A-, and B-type cyclins, reaching maximum expression at 6 h.

The exceptionally high synchrony and resolution in our analysis with meristematic cells arrested in proliferation in the dark, and their reentry into the cell cycle triggered by light, allowed us to identify specific clusters of cell cycle regulators associated with G1 arrest at 0 h (e.g., Siamese); early G1, peaking at 1 h (e.g., Cell Division Cycle6 [CDC6] and Origin Recognition Complex4 [ORC4]); mid G1, peaking at 2 h (e.g., Breast Cancer–Associated Ring and Mini Chromosome Maintenance7 [MCM7]); late G1, peaking at 2 to 6 h (e.g., MCM3 and ORC1a); both S-phase and mitosis, being maximum at 6 h among our sampled time points (e.g., CYCB1;1 and CYCA3;1); and exit from mitosis (mitosis-G1), peaking at 6 to 24 h (e.g., CDC20 and APC6). CYCD3;1, was only elevated at 24 to 48 h. Interestingly, during synchronization of cultured cells, CYCD3;1 was also found to peak in expression at the time of a second cell cycle (Menges et al., 2005).

Light is known to promote the endocycle in the hypocotyl primarily through PHYTOCHROME B and COP1 (Gendreau et al., 1998). Postembryonically, cotyledons undergo detectable but limited amounts of mitosis, with the bulk of cotyledon growth in light involving cell enlargement. This appears to correlate with cycles of endoreduplication (Stoynova-Bakalova et al., 2004).

We found that light activates cell proliferation in the shoot apex and endoreduplication in the cotyledons; thus, the same signal can trigger distinct cell cycle programs in the two organs. It is thought that the switch from cell proliferation to endoreduplication is characterized by the downregulation of G2-to-mitosis CDK activity and by an oscillation of G1-to-S CDK to allow the licensing of replication origin (De Veylder et al., 2007). Light stimulated, in both organs, the expression of largely similar groups of cell cycle genes, including D-, A-, and B-type cyclins and CDKB, all with maximal expression observed at 6 h. However, in the cotyledon, this response was quantitatively different: the activation of these genes was slower and showed lower amplitude than in the shoot apex. The expression of CDK inhibitors is known to regulate the exit to endocycle in a dose-dependent manner (De Veylder et al., 2007). We found that KRP1, which was described to be expressed in tissues undergoing endoreduplication (Ormenese et al., 2004), is more highly expressed in the cotyledon, while it is downregulated by light in the shoot apex. Thus, the transcriptional regulation of KRP1 could be one of the factors that determine tissue-specific cell cycle programs.

Photomorphogenic Regulators as Cell Cycle Control Factors

The *det* and *cop* mutants have uncovered the light signal–dependent proteolysis of transcriptional regulators as a central mechanism in photomorphogenesis. However, the COP and DET proteins are not unique to plants and are not only dedicated to light signaling but are recruited to regulate a wide array of biological processes in eukaryotes (Sullivan et al., 2003; Wei and Deng, 2003). In plants, the best characterized light-dependent target of the COP1- and CSN-mediated proteolysis is the HY5 transcription factor, but in *Drosophila*, CSN regulates cell proliferation by targeting cyclin E for degradation (Doronkin et al., 2003). In *Arabidopsis*, E2FC stability was also shown to be regulated by the SCF^{SKP2} E3 ubiqutin ligase complex: it is stable in the dark and rapidly turned over in the light (del Pozo et al., 2002). We found a similar and rapid destabilization of E2FC when dark-grown seedlings were transferred to light, while in seedlings in continuous light, two distinct E2FC forms became apparent. The origin of these forms is as yet unknown. However, the silencing of CSN5 mimics the transfer from dark to light, while mutants *det1* and *cop1* have E2FC forms that mimic the light-grown state, suggesting that E2FC is controlled by these signaling mechanisms. E2FC is a negative regulator of cell proliferation (Gutierrez, 2005), while E2FA is associated with S-phase control (De Veylder et al., 2002) and endoreduplication and E2FB is associated with the regulation of cell proliferation both at the G1- to S- and G2- to mitosis phases (Magyar et al., 2005). We previously established that E2FB is an unstable protein and that its turnover is regulated by the plant hormone auxin (Magyar et al., 2005). Here, we show that light also increases E2FB protein level and that this is dependent on CSN5 and COP1. Collectively, light alters the balance of the two E2F transcription factors, E2FC and E2FB, with opposing function in the regulation of cell proliferation, and this could be an important element in the program of derepression of meristem growth.

RBR1 is recruited to specific genes through the E2Fs and thereby represses E2F function directly or through the association with chromatin-modifying complexes. Important recent findings show that RBR1 regulates the switch between proliferation and differentiation and that CDK-mediated phosphorylation and inactivation of RBR1 is a sensitive measure of mitogenic signal inputs to this switch (De Veylder et al., 2007). In the root meristem, local reduction of RBR is sufficient to cause an increase in the number of stem cells, while overexpression of RBR dissipates the stem cell niche by triggering differentiation (Wildwater et al., 2005). Similarly, in the shoot apical meristem, local induction of RBR results in the occurrence of differentiation, as shown by the vacuolation of cells and the development of the photosynthetic apparatus (Wyrzykowska et al., 2006), two processes whose underlying transcriptional program took place in leaf primordia after 24 h in the light (this study). These striking parallels further suggest central roles of photomorphogenic regulators in the regulation of core cell cycle genes.

Time-resolved expression data are key to uncover underlying genetic regulatory networks (Bolouri and Davidson, 2002), so this environmentally switched shoot meristem activation data set may constitute one basis on which to start to build a leaf developmental network.

METHODS

Plant Material and Growth Conditions

Wild-type *Arabidopsis thaliana* plants belonged to the Landsberg *erecta* (L*er*) ecotype. The *hy1-1* mutant (Koornneef et al., 1980; Muramoto et al., 1999) in the L*er* background was obtained from the Nottingham Arabidopsis Stock Centre. To generate the triple photoreceptor mutant and its double mutant combinations, the double mutant between *hy4-1* (Koornneef et al., 1980; Ahmad and Cashmore, 1993) and *cry2/fha-1* (Guo et al., 1998) in L*er* was crossed to *hy1-1*, and each mutant combination was recovered in the progeny by a combination of phenotypic and PCR assays, as described previously (Weston et al., 2000). pCYCB;1:DB-GUS was kindly provided by Peter Doerner (University of Edinburgh), while pCYCD3;1:GUS was described previously (Masubelele et al., 2005). The *det1-1* mutant (Chory et al., 1989) was obtained from the Nottingham Arabidopsis Stock Centre. The *cop1-4* mutant (Deng et al., 1991) was a gift of J. Gray (University of Cambridge). Both of these mutants are in the Columbia (Col) background, and Col wild type was used as a control in experiments that included them.

Seedlings were grown on agar-solidified Murashige and Skoog medium, under continuous 100 $\mu mol \cdot m^{-2} \cdot s^{-1}$ fluorescent cool-white light, on horizontal plates in the absence or presence of 1% sucrose, and plants were grown on soil under 16-h 180 $\mu mol \cdot m^{-2} \cdot s^{-1}$ fluorescent white light photoperiods, all at 21°C, as described previously (Vinti et al., 2000). Seedlings for histochemistry or microarray analysis were raised in the absence of sugar by exposing sterilized, 3-d-stratified seeds to 30 min of white light before placing them in a dark incubator for 3 d, at which time they were transferred to white light.

Microscopy and Histochemical Observation

Histochemical GUS assays took place on seedlings harvested and fixed in TBS GUS buffer (100 mM Tris and 50 mM NaCl, pH 7.5) with 0.4% formaldehyde for 30 min at 4°C. Harvest and fixation of dark-grown seedlings took place under a green safelight (Vinti et al., 2000). After fixation, staining was performed for 12 h, followed by clearing in an increasing (25 to

100%) ethanol series, rehydration in a decreasing ethanol series, and mounting on microscope slides in Hoyer's solution, as described (Masubelele et al., 2005). Digital images were recorded using a Nikon SMZ1500 stereomicroscope equipped with a Nikon DXM1200 camera.

Preparation of Shoot Apex and Cotyledon Samples and Microarray Hybridizations

After sterilization, stratification, and exposure to light for 30 min to induce germination, plates were incubated in the dark for 72 h, then transferred to light and harvested at 0, 1, 2, 6, 24, 48, and 72 h after the transfer. Seedlings were harvested in <1 min per plate, immersed in RNA*later* (Ambion) for 1 h (the harvesting and immersion being under green safelight for the time 0 sample), and stored at 4°C. Within 1 week, seedlings were dissected on a chilled platform with a Nikon stereomicroscope by slicing below the meristem and at the base of each cotyledon (shoot apex samples) or near the base and tip of each cotyledon (cotyledon samples), before flash-freezing and storing at −80°C. Further details on the preparation of RNA, the microarray hybridizations, and the quality controls on the resulting data are given as the Supplemental Methods online.

Microarray Analysis and Data Processing

Microarray data analysis was performed by a combination of spreadsheet arithmetic calculations and the open-source Bioconductor software suite (http://www.bioconductor.org/). Three separate background correction, normalization, and summarization procedures were used: MAS5 (Affymetrix), gcRMA (Wu et al., 2004), and VSN (Huber et al., 2002). In order to determine the differentially expressed genes, a two-way ANOVA test (tissue and time, and the interaction between them) was applied on each normalized expression set for 0, 1, and 6 h (i.e., those times when replicated samples existed for both tissues). Further details for the microarray analysis, the two strategies to identify groups of functionally informative, corregulated genes, and their functional classification can be found in the Supplemental Methods online.

Determination of DNA Contents

Samples equivalent to those used for microarray analysis were generated, except that the full range of time points (0 to 72 h after transfer to light) was used for both shoot apex and cotyledon samples and that the number of seedlings per sample was one-tenth of that used for microarray. Samples were finely chopped in buffer (Galbraith et al., 1991) to release nuclei and filtered before staining with 5 μg/mL 4′,6-diamidino-2-phenylindole. The nuclear DNA content distribution was analyzed with a BRYTE HS (Bio-Rad) or a PAS2 (Partec) flow cytometer. The measurements were performed twice, and a third time at 0 h, 6 h, and subsequent time points, with comparable results. Results from one representative experiment are shown as percentages (Figure 8) and from another as fluorescence intensity distribution plots (see Supplemental Figure 10 online).

qPCR

Aliquots of one series of RNA samples used for microarray were also tested for the expression of representative genes by qPCR. cDNA synthesis was performed using a QuantiTect reverse transcription kit (Qiagen), which includes a genomic DNA removal step, according to the manufacturer's instructions. Real-time amplification in the presence of SYBR Green was performed using a BioScript PCR kit (Bioline) according to the manufacturer's instructions in a Rotor-Gene 6000 apparatus (Corbett Life Science). All reactions took place in triplicate. Levels of each transcript relative to the *ACT2* control gene were quantified by the method of Pfaffl (2001) using the shoot apex 0 sample as a reference. PCR primer pairs were designed in Primer3 (http://frodo.wi.mit.edu/), using settings designed to minimize the occurrence of primer dimers, and are given as Supplemental Table 6 online. Each amplicon was cloned into pGEM-T (Promega) and sequenced to confirm its identity.

Immunoblot Analysis of Seedlings and Cell Suspensions

Seedlings of *Arabidopsis* Col wild type, *det1-1*, and *cop1-4* were grown as for microarray experiments, except for a duration of 5 or 7 d in continuous darkness or white light as indicated. Preparation of whole seedling protein extracts and immunoblotting were performed as described previously (Magyar et al., 1997). Quantitation of immunoblots was performed using ImageQuant (Amersham Biosciences). *Arabidopsis* leaf protoplasts were prepared and transformed with constructs for the expression of HA-tagged forms of E2FB and E2FC as described (Magyar et al., 2005). Antibodies against E2FB, CDKA (against the conserved PSTAIRE domain), and HA tag were as described (Magyar et al., 2005).

The antibody against E2FC was commercially raised in chicken against two peptide antigens, of sequences 5′-QITQKVQKSRKNHRIQC-3′ and 5′-CYKGDSAETSDKLGNE-3′, and affinity-purified (Agrisera) before use. The RNAi construct for CSN5A (AJH1; At1g22920) was generated by PCR amplification from a cDNA clone containing the complete open reading frame of AJH1 and then subcloned into an RNAi vector containing Gateway sites (Karimi et al., 2002). The efficacy of the silencing was confirmed by coexpressing this construct together with a myc-tagged version of CSN5A. The myc-tagged version of CSN5A was generated according to Magyar et al. (2000).

Data Accession

The microarray data in this study are deposited in the Nottingham Arabidopsis Stock Centre (www.Arabidopsis.info) under reference NASCARRAYS-426.

Accession Numbers

Sequence data from this article can be found in the Arabidopsis Genome Initiative database under the following accession numbers: *HY1* (At2g26670), *CRY1* (At4g08920), *CRY2* (At1g04400), *E2FB* (At5g22220), and *E2FC* (At1g47870). Additional accession numbers can be found in Supplemental Table 6 online.

Supplemental Data

The following materials are available in the online version of this article.

Supplemental Figure 1. RNA Quality Control for Each Sample, Clustering Tree Showing Relatedness between Time Point and Replicate Samples, Scatterplots Showing Similarity between Replicates, and Strategy Employed in the Microarray Sample Dissection and Data/Pathway Analysis.

Supplemental Figure 2. Expression Levels of Differentially Expressed Genes Fitting Supervised Patterns, and Overrepresentation of Functional Categories for Each Group of Genes.

Supplemental Figure 3. Overlap between Genes Identified as Differentially Expressed in This Study and Previously Known Light-Regulated Genes or Genes Differentially Expressed in Seedling or Embryo Regions.

Supplemental Figure 4. Expression Heat Map for MAPK Proteins and PP2C Protein Phosphatases.

Supplemental Figure 5. Overrepresentation/Underrepresentation Probabilities of Every Family of Transcription Factors among Robust, Differentially Expressed Genes, and Expression Heat Maps of ARF and GRF Families.

Supplemental Figure 6. Expression Heat Map of Transcription Factors Belonging to the GATA and Myb Families.

Supplemental Figure 7. Expression Heat Maps for Genes Positively or Negatively Regulated by the Hormones Abscisic Acid and Brassinolide.

Supplemental Figure 8. Expression Heat Maps for Genes Involved in Cell Wall Modification and Extensibility and in Turgor Generation.

Supplemental Figure 9. Expression Heat Maps for Genes Previously Identified as Associated with S-Phase and Mitosis or with Proliferation in Developing Leaves and Roots.

Supplemental Figure 10. Flow-Cytometric Distribution of Ploidy Levels in Shoot Apex and Cotyledon Samples at Selected Time Points.

Supplemental Figure 11. Expression Heat Maps for Genes Previously Identified as Positively or Negatively Regulated by the Pair of Transcription Factors E2FA/DPa.

Supplemental Figure 12. Expression Heat Map for Chloroplast Biogenesis and Photosynthesis-Related Genes.

Supplemental Table 1. Expression Values (Extracted by the gcRMA Algorithm) for All Genes in the ATH1 Array.

Supplemental Table 2. List of All Differentially Expressed Genes, Selected as Indicated in the Text, with Expression Values (gcRMA), Absolute and Mean-Centered Averages, and P Value of the ANOVA (for Tissue, Time, or Interaction between Them) for Each Gene (The Genes Are Grouped in Clusters Identified by the K-Means Algorithm).

Supplemental Table 3. Lists of Differentially Expressed Genes That Fit Selected Supervised Expression Patterns, and Expression Values for Each Gene (gcRMA) and Absolute and Mean-Centered Averages.

Supplemental Table 4. Selected GO Terms among the Supervised Patterns Shown in Supplemental Figure 2.

Supplemental Table 5. Lists of Genes in Each of the Individual Biological Processes Analyzed in This Study, Together with Their Expression Values (gcRMA), Averages, and Fold Induction by Light (at 1 and 6 h), in Shoot Apex or Cotyledon Samples.

Supplemental Table 6. Primers Used for qPCR.

Supplemental Methods. Sample Preparation, Microarray Hybridizations, and Parallel Strategies for Microarray Analysis and Gene Functional Classification.

ACKNOWLEDGMENTS

We are indebted to Véronique Boudolf (Flanders Institute of Biotechnology) for the clone containing AJH1; to the MapMan team (Max Planck Institute, Golm) and M. Schmid (Max Planck Institute, Tübingen) for making available lists of gene functional classifications; to the bioinformatics team at the Nottingham Arabidopsis Stock Centre; and to the members of the Flanders Institute of Biotechnology, participants in the European Union Growth, Vigour, Environment project, and Paul Devlin for helpful discussions. This work was funded in part by the European Union GVE project (Grant QLK5-2001) and by the Biotechnology and Biological Science Research Council of the United Kingdom (Grant BBS/B/13314).

Received November 21, 2007; revised February 19, 2008; accepted March 24, 2008; published April 18, 2008.

REFERENCES

Aguilar-Martinez, J.A., Poza-Carrion, C., and Cubas, P. (2007). Arabidopsis BRANCHED1 acts as an integrator of branching signals within axillary buds. Plant Cell **19:** 458–472.

Ahmad, M., and Cashmore, A.R. (1993). HY4 gene of *A. thaliana* encodes a protein with characteristics of a blue-light photoreceptor. Nature **366:** 162–166.

Alabadi, D., Oyama, T., Yanovsky, M.J., Harmon, F.G., Mas, P., and Kay, S.A. (2001). Reciprocal regulation between TOC1 and LHY/CCA1 within the Arabidopsis circadian clock. Science **293:** 880–883.

Beemster, G.T., De Veylder, L., Vercruysse, S., West, G., Rombaut, D., Van Hummelen, P., Galichet, A., Gruissem, W., Inze, D., and Vuylsteke, M. (2005). Genome-wide analysis of gene expression profiles associated with cell cycle transitions in growing organs of Arabidopsis. Plant Physiol. **138:** 734–743.

Bolouri, H., and Davidson, E.H. (2002). Modeling transcriptional regulatory networks. Bioessays **24:** 1118–1129.

Chory, J., Peto, C., Feinbaum, R., Pratt, L., and Ausubel, F. (1989). *Arabidopsis thaliana* mutant that develops as a light-grown plant in the absence of light. Cell **58:** 991–999.

Chory, J., Reinecke, D., Sim, S., Washburn, T., and Brenner, M. (1994). A role for cytokinins in de-etiolation in Arabidopsis—*det* mutants have an altered response to cytokinins. Plant Physiol. **104:** 339–347.

Clay, N.K., and Nelson, T. (2002). VH1, a provascular cell-specific receptor kinase that influences leaf cell patterns in Arabidopsis. Plant Cell **14:** 2707–2722.

Colon-Carmona, A., You, R., Haimovitch-Gal, T., and Doerner, P. (1999). Technical advance: Spatio-temporal analysis of mitotic activity with a labile cyclin-GUS fusion protein. Plant J. **20:** 503–508.

Cosgrove, D.J. (2005). Growth of the plant cell wall. Nat. Rev. Mol. Cell Biol. **6:** 850–861.

del Pozo, J.C., Boniotti, M.B., and Gutierrez, C. (2002). Arabidopsis E2Fc functions in cell division and is degraded by the ubiquitin-SCF^{AtSKP2} pathway in response to light. Plant Cell **14:** 3057–3071.

del Pozo, J.C., Diaz-Trivino, S., Cisneros, N., and Gutierrez, C. (2006). The balance between cell division and endoreplication depends on E2FC-DPB, transcription factors regulated by the ubiquitin-$SCF^{AtSKP2A}$ pathway in *Arabidopsis.* Plant Cell **18:** 2224–2235.

Deng, X.W., Caspar, T., and Quail, P.H. (1991). COP1—A regulatory locus involved in light-controlled development and gene-expression in Arabidopsis. Genes Dev. **5:** 1172–1182.

de Reuille, P.B., Bohn-Courseau, I., Ljung, K., Morin, H., Carraro, N., Godin, C., and Traas, J. (2006). Computer simulations reveal properties of the cell-cell signaling network at the shoot apex in Arabidopsis. Proc. Natl. Acad. Sci. USA **103:** 1627–1632.

De Veylder, L., Beeckman, T., Beemster, G., de Almeida Engler, J., Ormenese, S., Maes, S., Naudts, M., Van Der Schueren, E., Jacqmard, A., Engler, G., and Inze, D. (2002). Control of proliferation, endoreduplication and differentiation by the *Arabidopsis* E2Fa-DPa transcription factor. EMBO J. **21:** 1360–1368.

De Veylder, L., Beeckman, T., and Inze, D. (2007). The ins and outs of the plant cell cycle. Nat. Rev. Mol. Cell Biol. **8:** 655–665.

Devlin, P.F., Yanovsky, M.J., and Kay, S.A. (2003). A genomic analysis of the shade avoidance response in Arabidopsis. Plant Physiol. **133:** 1617–1629.

Dewitte, W., Riou-Khamlichi, C., Scofield, S., Healy, J.M., Jacqmard, A., Kilby, N.J., and Murray, J.A. (2003). Altered cell cycle distribution, hyperplasia, and inhibited differentiation in Arabidopsis caused by the D-type cyclin CYCD3. Plant Cell **15:** 79–92.

Dievart, A., and Clark, S.E. (2004). LRR-containing receptors regulating plant development and defense. Development **131:** 251–261.

Doronkin, S., Djagaeva, I., and Beckendorf, S.K. (2003). The COP9 signalosome promotes degradation of cyclin E during early Drosophila oogenesis. Dev. Cell **4:** 699–710.

Du, W., and Pogoriler, J. (2006). Retinoblastoma family genes. Oncogene **25:** 5190–5200.

Edwards, K.D., Anderson, P.E., Hall, A., Salathia, N.S., Locke, J.C., Lynn, J.R., Straume, M., Smith, J.Q., and Millar, A.J. (2006). FLOWERING LOCUS C mediates natural variation in the high-temperature response of the Arabidopsis circadian clock. Plant Cell **18:** 639–650.

Eyuboglu, B., Pfister, K., Haberer, G., Chevalier, D., Fuchs, A., Mayer, K.F.X., and Schneitz, K. (2007). Molecular characterisation of the STRUBBELIG-RECEPTOR FAMILY of genes encoding putative leucine-rich repeat receptor-like kinases in *Arabidopsis thaliana.* BMC Plant Biol. **7:**16.

Fitter, D.W., Martin, D.J., Copley, M.J., Scotland, R.W., and Langdale, J.A. (2002). GLK gene pairs regulate chloroplast development in diverse plant species. Plant J. **31:** 713–727.

Fleming, A.J. (2006). The co-ordination of cell division, differentiation and morphogenesis in the shoot apical meristem: A perspective. J. Exp. Bot. **57:** 25–32.

Fleury, D., et al. (2007). The *Arabidopsis thaliana* homolog of yeast BRE1 has a function in cell cycle regulation during early leaf and root growth. Plant Cell **19:** 417–432.

Foo, E., Ross, J.J., Davies, N.W., Reid, J.B., and Weller, J.L. (2006). A role for ethylene in the phytochrome-mediated control of vegetative development. Plant J. **46:** 911–921.

Galbraith, D.W., Harkins, K.R., and Knapp, S. (1991). Systemic endopolyploidy in *Arabidopsis thaliana.* Plant Physiol. **96:** 985–989.

Gendreau, E., Hofte, H., Grandjean, O., Brown, S., and Traas, J. (1998). Phytochrome controls the number of endoreduplication cycles in the *Arabidopsis thaliana* hypocotyl. Plant J. **13:** 221–230.

Gil, P., Dewey, E., Friml, J., Zhao, Y., Snowden, K.C., Putterill, J., Palme, K., Estelle, M., and Chory, J. (2001). BIG: A calossin-like protein required for polar auxin transport in Arabidopsis. Genes Dev. **15:** 1985–1997.

Guo, H., Yang, H., Mockler, T.C., and Lin, C. (1998). Regulation of flowering time by Arabidopsis photoreceptors. Science **279:** 1360–1363.

Gutierrez, C. (2005). Coupling cell proliferation and development in plants. Nat. Cell Biol. **7:** 535–541.

Harmer, S.L., Hogenesch, J.B., Straume, M., Chang, H.S., Han, B., Zhu, T., Wang, X., Kreps, J.A., and Kay, S.A. (2000). Orchestrated transcription of key pathways in Arabidopsis by the circadian clock. Science **290:** 2110–2113.

Hay, A., Kaur, H., Phillips, A., Hedden, P., Hake, S., and Tsiantis, M. (2002). The gibberellin pathway mediates KNOTTED1-type homeobox function in plants with different body plans. Curr. Biol. **12:** 1557–1565.

Higuchi, M., et al. (2004). In planta functions of the Arabidopsis cytokinin receptor family. Proc. Natl. Acad. Sci. USA **101:** 8821–8826.

Hoecker, U., Tepperman, J.M., and Quail, P.H. (1999). SPA1, a WD-repeat protein specific to phytochrome A signal transduction. Science **284:** 496–499.

Holm, M., Ma, L.G., Qu, L.J., and Deng, X.W. (2002). Two interacting bZIP proteins are direct targets of COP1-mediated control of light-dependent gene expression in Arabidopsis. Genes Dev. **16:** 1247–1259.

Huber, W., von Heydebreck, A., Sultmann, H., Poustka, A., and Vingron, M. (2002). Variance stabilization applied to microarray data calibration and to the quantification of differential expression. Bioinformatics **18** (suppl. 1): S96–S104.

Jasinski, S., Piazza, P., Craft, J., Hay, A., Woolley, L., Rieu, I., Phillips, A., Hedden, P., and Tsiantis, M. (2005). KNOX action in Arabidopsis is mediated by coordinate regulation of cytokinin and gibberellin activities. Curr. Biol. **15:** 1560–1565.

Jiao, Y., Lau, O.S., and Deng, X.W. (2007). Light-regulated transcriptional networks in higher plants. Nat. Rev. Genet. **8:** 217–230.

Karimi, M., Inze, D., and Depicker, A. (2002). GATEWAY((TM)) vectors for Agrobacterium-mediated plant transformation. Trends Plant Sci. **7:** 193–195.

Kepinski, S. (2006). Integrating hormone signaling and patterning mechanisms in plant development. Curr. Opin. Plant Biol. **9:** 28–34.

Khanna, R., Shen, Y., Toledo-Ortiz, G., Kikis, E.A., Johannesson, H., Hwang, Y.S., and Quail, P.H. (2006). Functional profiling reveals that only a small number of phytochrome-regulated early-response genes in Arabidopsis are necessary for optimal deetiolation. Plant Cell **18:** 2157–2171.

Koornneef, M., Rolff, E., and Spruit, C.J.P. (1980). Genetic-control of light-inhibited hypocotyl elongation in *Arabidopsis thaliana* (L) Heynh. Z. Pflanzenphysiol. **100:** 147–160.

Koyama, T., Furutani, M., Tasaka, M., and Ohme-Takagi, M. (2007). TCP transcription factors control the morphology of shoot lateral organs via negative regulation of the expression of boundary-specific genes in Arabidopsis. Plant Cell **19:** 473–484.

Leibfried, A., To, J.P., Busch, W., Stehling, S., Kehle, A., Demar, M., Kieber, J.J., and Lohmann, J.U. (2005). WUSCHEL controls meristem function by direct regulation of cytokinin-inducible response regulators. Nature **438:** 1172–1175.

Li, C., Potuschak, T., Colon-Carmona, A., Gutierrez, R.A., and Doerner, P. (2005). Arabidopsis TCP20 links regulation of growth and cell division control pathways. Proc. Natl. Acad. Sci. USA **102:** 12978–12983.

Li, J., Nagpal, P., Vitart, V., McMorris, T.C., and Chory, J. (1996). A role for brassinosteroids in light-dependent development of Arabidopsis. Science **272:** 398–401.

Ma, L., Gao, Y., Qu, L., Chen, Z., Li, J., Zhao, H., and Deng, X.W. (2002). Genomic evidence for COP1 as a repressor of light-regulated gene expression and development in Arabidopsis. Plant Cell **14:** 2383–2398.

Ma, L., Li, J., Qu, L., Hager, J., Chen, Z., Zhao, H., and Deng, X.W. (2001). Light control of Arabidopsis development entails coordinated regulation of genome expression and cellular pathways. Plant Cell **13:** 2589–2607.

Ma, L., Sun, N., Liu, X., Jiao, Y., Zhao, H., and Deng, X.W. (2005). Organ-specific expression of Arabidopsis genome during development. Plant Physiol. **138:** 80–91.

Magyar, Z., Atanassova, A., De Veylder, L., Rombauts, S., and Inze, D. (2000). Characterization of two distinct DP-related genes from *Arabidopsis thaliana.* FEBS Lett. **486:** 79–87.

Magyar, Z., De Veylder, L., Atanassova, A., Bako, L., Inze, D., and Bogre, L. (2005). The role of the Arabidopsis E2FB transcription factor in regulating auxin-dependent cell division. Plant Cell **17:** 2527–2541.

Magyar, Z., et al. (1997). Cell cycle phase specificity of putative cyclin-dependent kinase variants in synchronized alfalfa cells. Plant Cell **9:** 223–235.

Mallappa, C., Yadav, V., Negi, P., and Chattopadhyay, S. (2006). A basic leucine zipper transcription factor, G-box-binding factor 1, regulates blue light-mediated photomorphogenic growth in Arabidopsis. J. Biol. Chem. **281:** 22190–22199.

Manfield, I.W., Devlin, P.F., Jen, C.H., Westhead, D.R., and Gilmartin, P.M. (2007). Conservation, convergence, and divergence of light-responsive, circadian-regulated, and tissue-specific expression patterns during evolution of the Arabidopsis GATA gene family. Plant Physiol. **143:** 941–958.

Masubelele, N.H., Dewitte, W., Menges, M., Maughan, S., Collins, C., Huntley, R., Nieuwland, J., Scofield, S., and Murray, J.A. (2005).

D-type cyclins activate division in the root apex to promote seed germination in Arabidopsis. Proc. Natl. Acad. Sci. USA **102:** 15694–15699.

Masuda, H.P., Ramos, G.B.A., de Almeida-Engler, J., Cabral, L.M., Coqueiro, V.M., Macrini, C.M.T., Ferreira, P.C.G., and Hemerly, A.S. (2004). Genome based identification and analysis of the pre-replicative complex of *Arabidopsis thaliana.* FEBS Lett. **574:** 192–202.

Mazzella, M.A., Cerdan, P.D., Staneloni, R.J., and Casal, J.J. (2001). Hierarchical coupling of phytochromes and cryptochromes reconciles stability and light modulation of Arabidopsis development. Development **128:** 2291–2299.

Menges, M., de Jager, S.M., Gruissem, W., and Murray, J.A. (2005). Global analysis of the core cell cycle regulators of Arabidopsis identifies novel genes, reveals multiple and highly specific profiles of expression and provides a coherent model for plant cell cycle control. Plant J. **41:** 546–566.

Moller, S.G., Ingles, P.J., and Whitelam, G. (2002). The cell biology of phytochrome signalling. New Phytol. **154:** 553–590.

Monte, E., Tepperman, J.M., Al-Sady, B., Kaczorowski, K.A., Alonso, J.M., Ecker, J.R., Li, X., Zhang, Y., and Quail, P.H. (2004). The phytochrome-interacting transcription factor, PIF3, acts early, selectively, and positively in light-induced chloroplast development. Proc. Natl. Acad. Sci. USA **101:** 16091–16098.

Muramoto, T., Kohchi, T., Yokota, A., Hwang, I., and Goodman, H.M. (1999). The Arabidopsis photomorphogenic mutant *hy1* is deficient in phytochrome chromophore biosynthesis as a result of a mutation in a plastid heme oxygenase. Plant Cell **11:** 335–348.

Nemhauser, J.L. (2008). Dawning of a new era: Photomorphogenesis as an integrated molecular network. Curr. Opin. Plant Biol. **11:** 4–8.

Nemhauser, J.L., Hong, F., and Chory, J. (2006). Different plant hormones regulate similar processes through largely nonoverlapping transcriptional responses. Cell **126:** 467–475.

Neufeld, T.P., and Edgar, B.A. (1998). Connections between growth and the cell cycle. Curr. Opin. Cell Biol. **10:** 784–790.

Ohgishi, M., Saji, K., Okada, K., and Sakai, T. (2004). Functional analysis of each blue light receptor, cry1, cry2, phot1, and phot2, by using combinatorial multiple mutants in Arabidopsis. Proc. Natl. Acad. Sci. USA **101:** 2223–2228.

Ormenese, S., de Almeida Engler, J., De Groodt, R., De Veylder, L., Inze, D., and Jacqmard, A. (2004). Analysis of the spatial expression pattern of seven Kip related proteins (KRPs) in the shoot apex of *Arabidopsis thaliana.* Ann. Bot. (Lond.) **93:** 575–580.

Ortega-Martinez, O., Pernas, M., Carol, R.J., and Dolan, L. (2007). Ethylene modulates stem cell division in the *Arabidopsis thaliana* root. Science **317:** 507–510.

Osterlund, M.T., Hardtke, C.S., Wei, N., and Deng, X.W. (2000). Targeted destabilization of HY5 during light-regulated development of Arabidopsis. Nature **405:** 462–466.

Pekker, I., Alvarez, J.P., and Eshed, Y. (2005). Auxin response factors mediate Arabidopsis organ asymmetry via modulation of KANADI activity. Plant Cell **17:** 2899–2910.

Pfaffl, M.W. (2001). A new mathematical model for relative quantification in real-time RT-PCR. Nucleic Acids Res. **29:** e45.

Shani, E., Yanai, O., and Ori, N. (2006). The role of hormones in shoot apical meristem function. Curr. Opin. Plant Biol. **9:** 484–489.

Sibout, R., Sukumar, P., Hettiarachchi, C., Holm, M., Muday, G.K., and Hardtke, C.S. (2006). Opposite root growth phenotypes of *hy5* versus *hy5 hyh* mutants correlate with increased constitutive auxin signaling. PLoS Genet **2:** 1898–1911.

Spencer, M.W., Casson, S.A., and Lindsey, K. (2007). Transcriptional profiling of the Arabidopsis embryo. Plant Physiol. **143:** 924–940.

Stoynova-Bakalova, E., Karanov, E., Petrov, P., and Hall, M.A. (2004). Cell division and cell expansion in cotyledons of Arabidopsis seedlings. New Phytol. **162:** 471–479.

Sullivan, J.A., Shirasu, K., and Deng, X.W. (2003). The diverse roles of ubiquitin and the 26S proteasome in the life of plants. Nat. Rev. Genet. **4:** 948–958.

Swarup, R., Perry, P., Hagenbeek, D., Van Der Straeten, D., Beemster, G.T., Sandberg, G., Bhalerao, R., Ljung, K., and Bennett, M.J. (2007). Ethylene upregulates auxin biosynthesis in Arabidopsis seedlings to enhance inhibition of root cell elongation. Plant Cell **19:** 2186–2196.

Tatematsu, K., Ward, S., Leyser, O., Kamiya, Y., and Nambara, E. (2005). Identification of cis-elements that regulate gene expression during initiation of axillary bud outgrowth in Arabidopsis. Plant Physiol. **138:** 757–766.

Tepperman, J.M., Hudson, M.E., Khanna, R., Zhu, T., Chang, S.H., Wang, X., and Quail, P.H. (2004). Expression profiling of *phyB* mutant demonstrates substantial contribution of other phytochromes to red-light-regulated gene expression during seedling de-etiolation. Plant J. **38:** 725–739.

Tepperman, J.M., Hwang, Y.S., and Quail, P.H. (2006). phyA dominates in transduction of red-light signals to rapidly responding genes at the initiation of Arabidopsis seedling de-etiolation. Plant J. **48:** 728–742.

Tepperman, J.M., Zhu, T., Chang, H.S., Wang, X., and Quail, P.H. (2001). Multiple transcription-factor genes are early targets of phytochrome A signaling. Proc. Natl. Acad. Sci. USA **98:** 9437–9442.

Tian, Q., Uhlir, N.J., and Reed, J.W. (2002). Arabidopsis SHY2/IAA3 inhibits auxin-regulated gene expression. Plant Cell **14:** 301–319.

Timmers, C., Sharma, N., Opavsky, R., Maiti, B., Wu, L., Wu, J., Orringer, D., Trikha, P., Saavedra, H.I., and Leone, G. (2007). E2f1, E2f2, and E2f3 control E2F target expression and cellular proliferation via a p53-dependent negative feedback loop. Mol. Cell. Biol. **27:** 65–78.

Tremousaygue, D., Garnier, L., Bardet, C., Dabos, P., Herve, C., and Lescure, B. (2003). Internal telomeric repeats and 'TCP domain' protein-binding sites co-operate to regulate gene expression in *Arabidopsis thaliana* cycling cells. Plant J. **33:** 957–966.

Vandepoele, K., Raes, J., De Veylder, L., Rouze, P., Rombauts, S., and Inze, D. (2002). Genome-wide analysis of core cell cycle genes in Arabidopsis. Plant Cell **14:** 903–916.

Vandepoele, K., Vlieghe, K., Florquin, K., Hennig, L., Beemster, G.T., Gruissem, W., Van de Peer, Y., Inze, D., and De Veylder, L. (2005). Genome-wide identification of potential plant E2F target genes. Plant Physiol. **139:** 316–328.

Vanneste, S., et al. (2005). Cell cycle progression in the pericycle is not sufficient for SOLITARY ROOT/IAA14-mediated lateral root initiation in *Arabidopsis thaliana.* Plant Cell **17:** 3035–3050.

Vinti, G., Hills, A., Campbell, S., Bowyer, J.R., Mochizuki, N., Chory, J., and Lopez-Juez, E. (2000). Interactions between *hy1* and *gun* mutants of Arabidopsis, and their implications for plastid/nuclear signalling. Plant J. **24:** 883–894.

Wei, N., and Deng, X.W. (2003). The COP9 signalosome. Annu. Rev. Cell Dev. Biol. **19:** 261–286.

Weston, E., Thorogood, K., Vinti, G., and Lopez-Juez, E. (2000). Light quantity controls leaf-cell and chloroplast development in *Arabidopsis thaliana* wild type and blue-light-perception mutants. Planta **211:** 807–815.

Whitelam, G., and Halliday, K. (2007). Light and Plant Development. (Oxford, UK: Blackwell).

Wildwater, M., Campilho, A., Perez-Perez, J.M., Heidstra, R., Blilou, I., Korthout, H., Chatterjee, J., Mariconti, L., Gruissem, W., and Scheres, B. (2005). The *RETINOBLASTOMA-RELATED* gene regulates stem cell maintenance in *Arabidopsis* roots. Cell **123:** 1337–1349.

Wu, Z.J., Irizarry, R.A., Gentleman, R., Martinez-Murillo, F., and Spencer, F. (2004). A model-based background adjustment for oligonucleotide expression arrays. J. Am. Stat. Assoc. **99:** 909–917.

Wyrzykowska, J., Schorderet, M., Pien, S., Gruissem, W., and Fleming, A.J. (2006). Induction of differentiation in the shoot apical meristem by transient overexpression of a retinoblastoma-related protein. Plant Physiol. **141:** 1338–1348.

Yamaguchi, S., Smith, M.W., Brown, R.G., Kamiya, Y., and Sun, T. (1998). Phytochrome regulation and differential expression of gibberellin 3beta-hydroxylase genes in germinating Arabidopsis seeds. Plant Cell **10:** 2115–2126.

Yang, J., and Wang, H. (2006). The central coiled-coil domain and carboxyl-terminal WD-repeat domain of Arabidopsis SPA1 are responsible for mediating repression of light signaling. Plant J. **47:** 564–576.

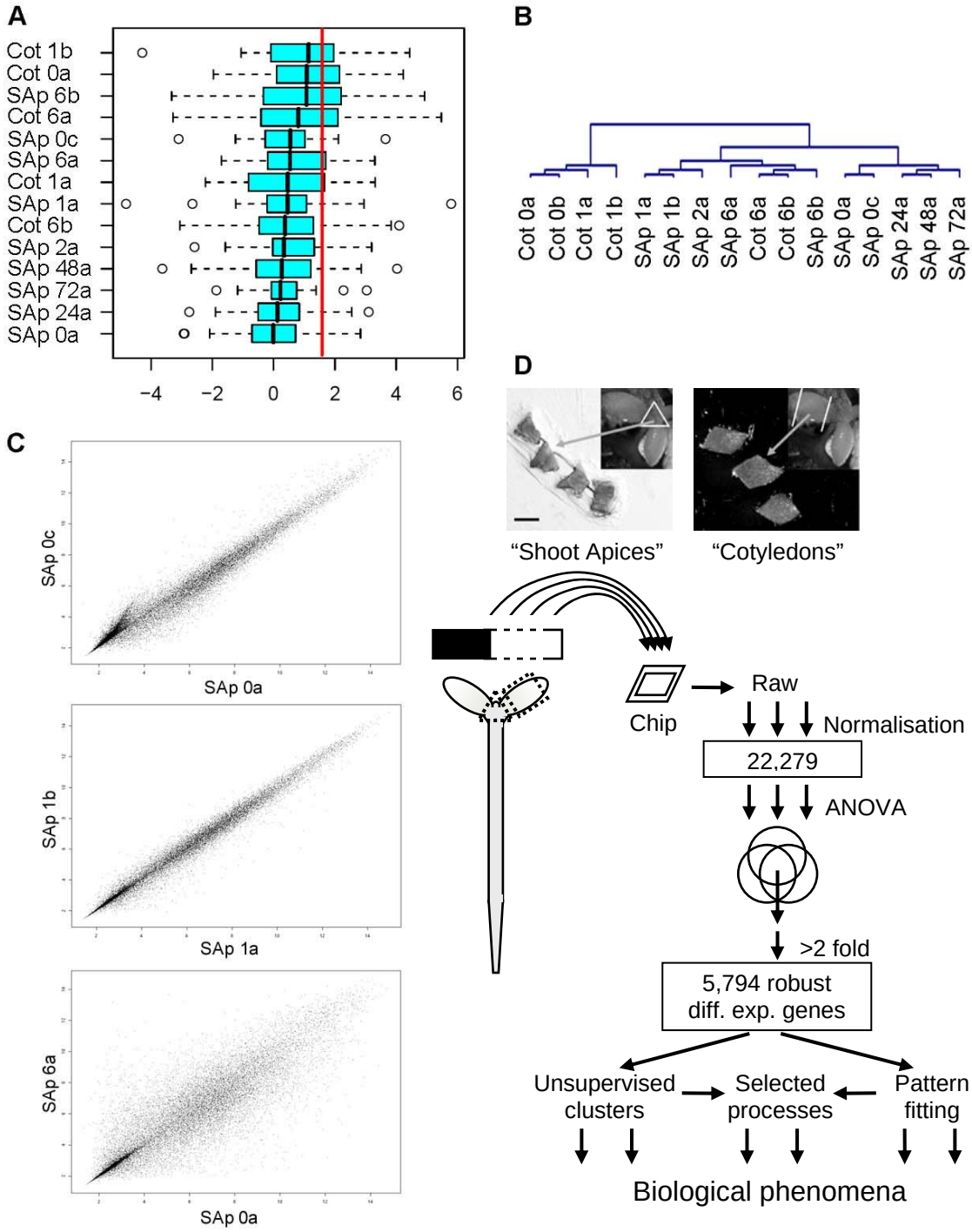

Supplemental Figure 1. (A) Control for RNA quality in each sample: $\log_2$(3′/5′) of Affymetrix housekeeping genes. Box plots showing the 25 and 75 percentiles. The red line indicates the recommended $\log_2(3)$ limit, to the left of which is undegraded RNA. (B) Hierarchical clustering tree (using Pearson correlation) of samples. The tree shows the similarity between replicates, the large but transient change between SAp 0 and early light samples, and the similarity between late light samples. (C) Example scatter plots of paired shoot apex samples, showing that high correlation between replicates and the spread when comparing different times. (D) Summary of the strategy used to identify pathways targeted by light signaling in shoot apices and cotyledons upon transition from dark to light. The panels at the top show the sample material. Scale bar: 200 μm.

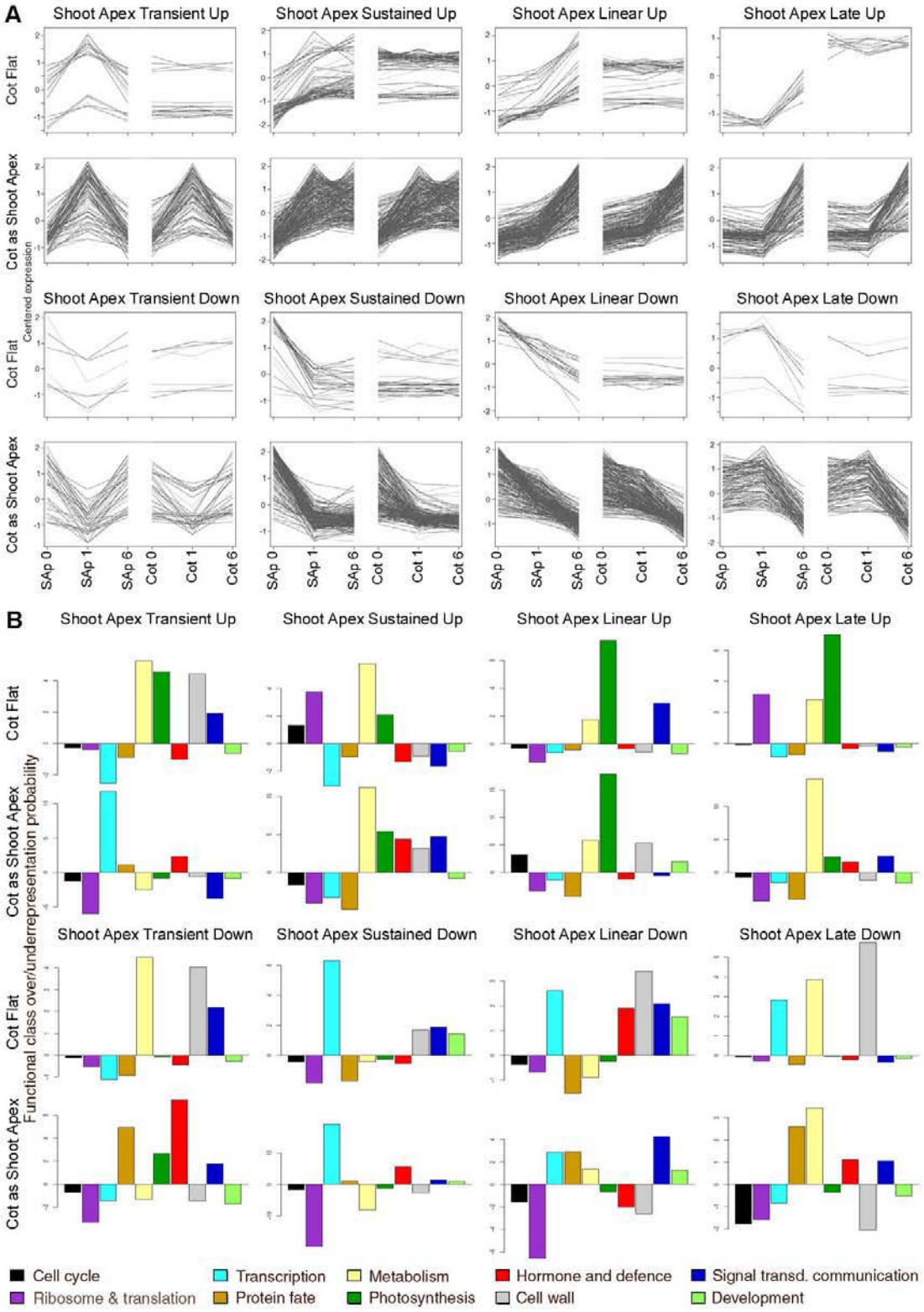

Supplemental Figure 2. (A) Expression levels of differentially expressed genes fitting one of sixteen, among eighty one possible, supervised patterns. (B) Histograms showing overrepresentation of selected functional categories for each group of genes.

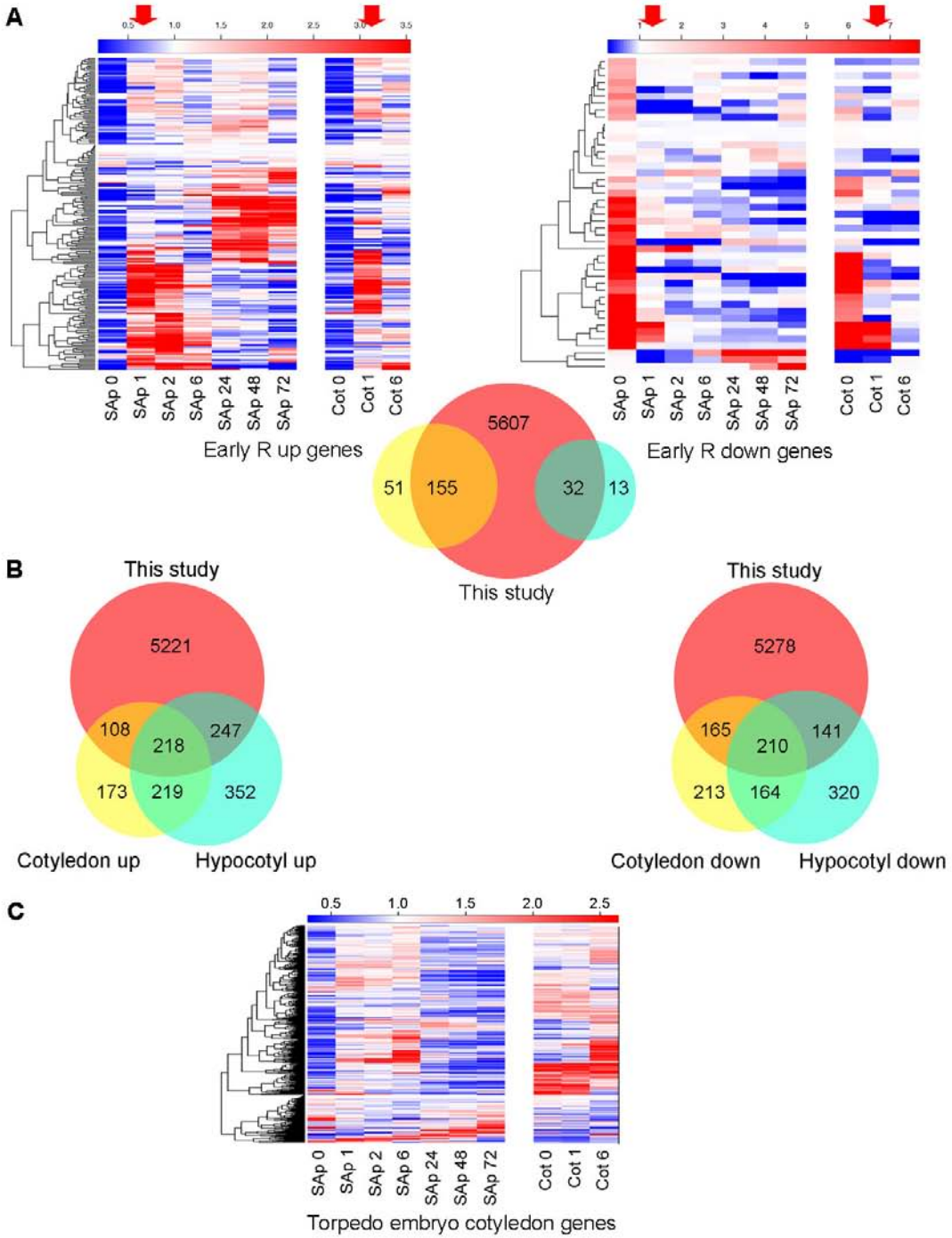

Supplemental Figure 3. Overlap between genes identified as differentially expressed in this study and previously-known light-regulated or embryo-differential genes. (A) Heatmap of expression levels (linear scale shown) in this study, of genes previously identified as robustly regulated in whole seedlings after one hour of red light (R) by Tepperman and (2006). The middle Venn diagram indicates the extent of overlap between genes rapidly up- or down-regulated and those identified as differentially expressed in our analysis. SAp: Shoot Apex. Cot: Cotyledon. (B) Venn diagrammes indicating the extent of overlap between this analysis and genes previously found to be differentially regulated in seedling organs (Ma et al. 2005). (C) Expression levels in our study of genes differentially expressed in torpedo-stage embryo cotyledon relative to embryo shoot meristem by Spencer et al. (2007), two substantial groups of which were constitutively expressed also in seedling cotyledons in the present study.

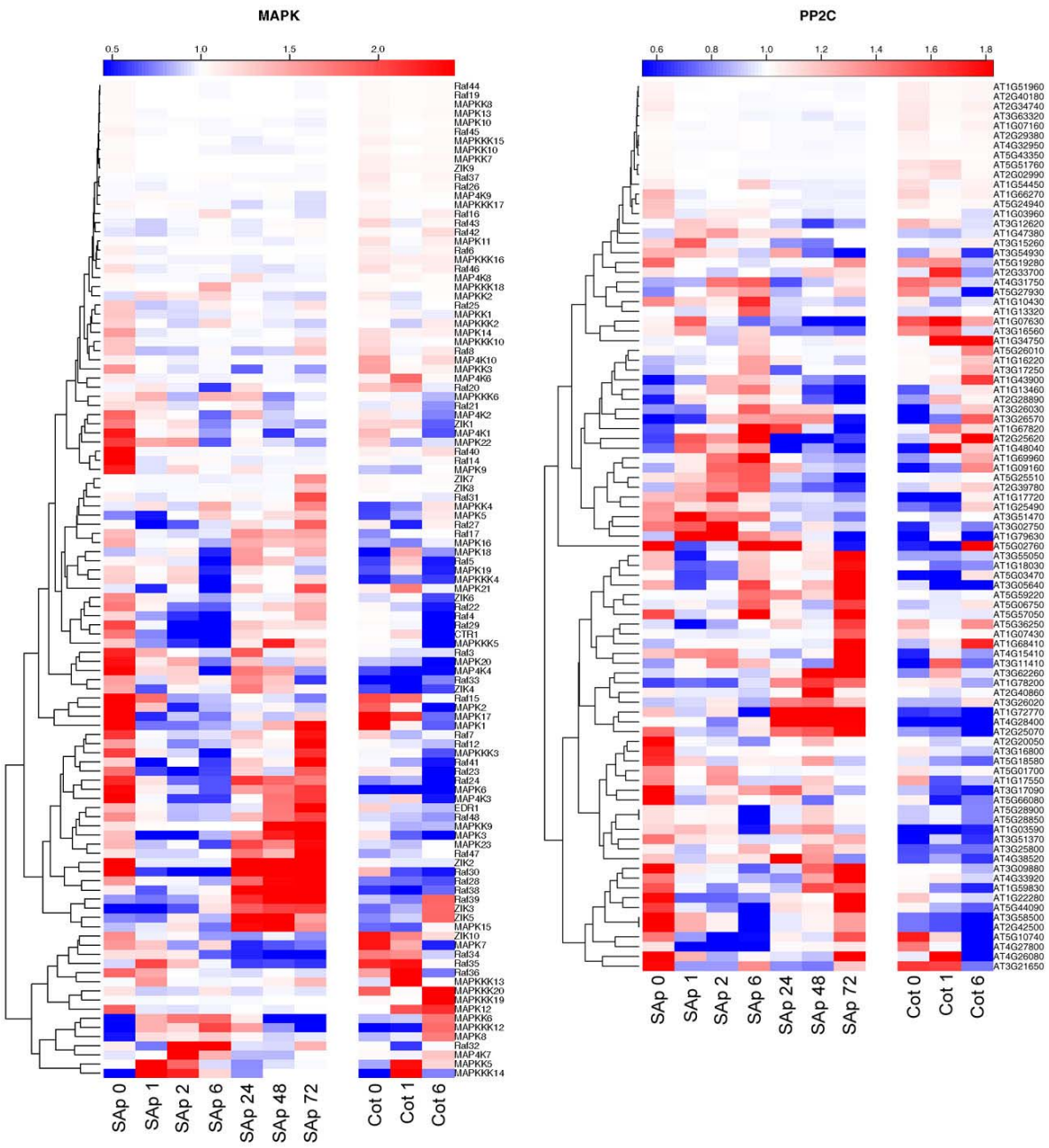

Supplemental Figure 4. Expression heatmap for mitogen-activated protein kinase (MAPK) proteins and PP2C protein phosphatases.

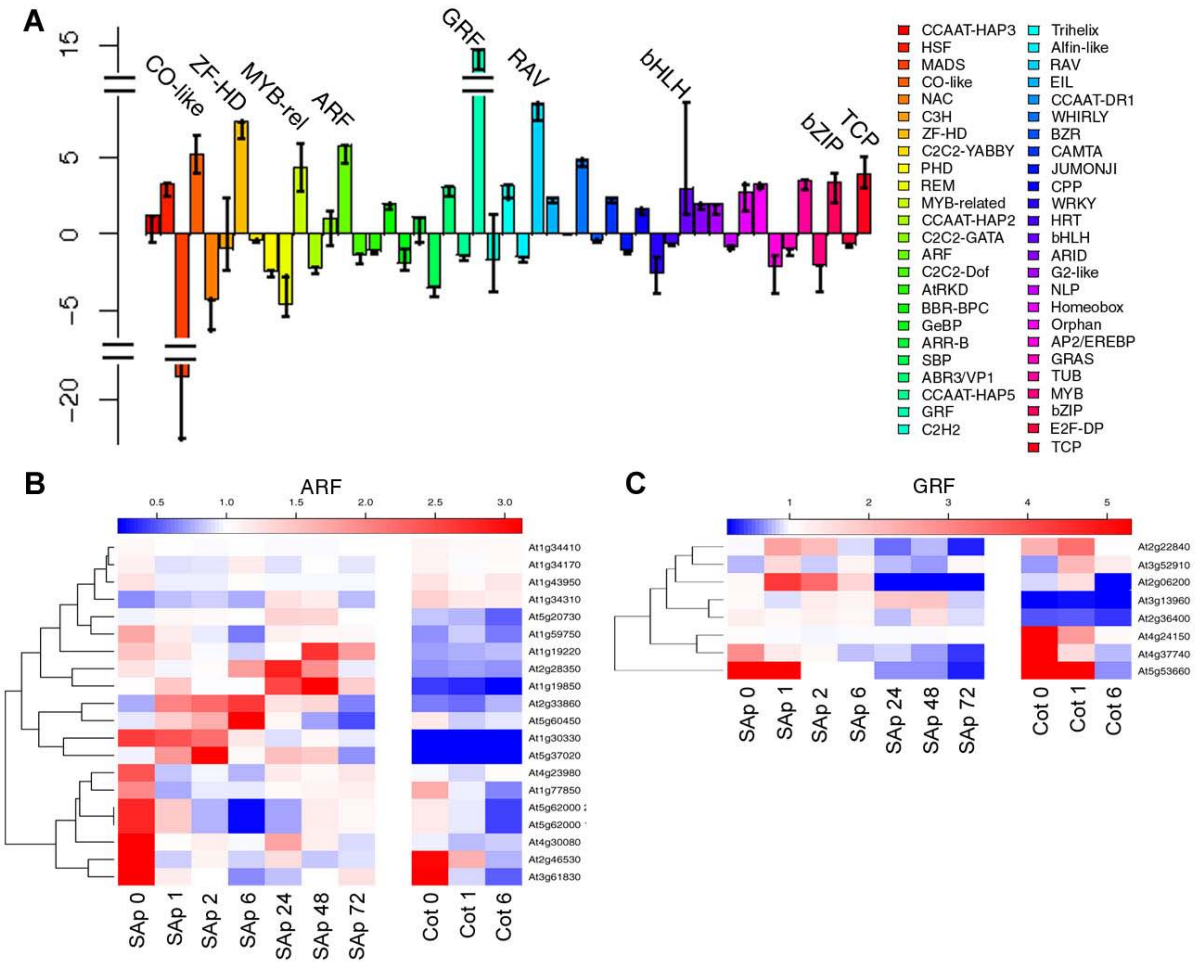

Supplemental Figure 5. (A) Over/under-representation probabilities of each family of transcription factors among robust, differentially-expressed genes. (B, C) Heatmaps of auxin response factor (ARF, B) and growth regulatory factor (GRF, C) transcription factor families.

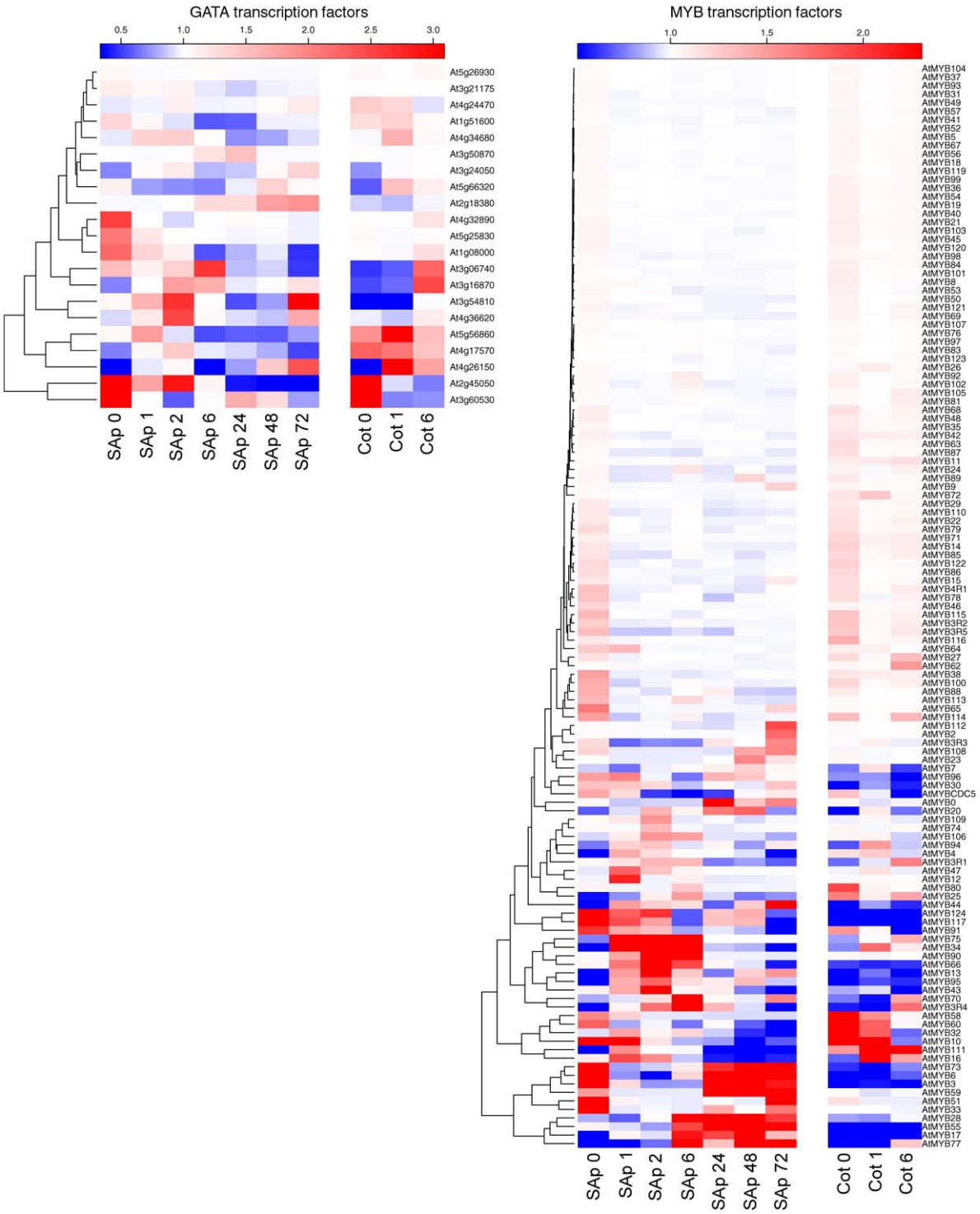

Supplemental Figure 6. Expression heatmap of transcription factors belonging to the GATA and Myb families.

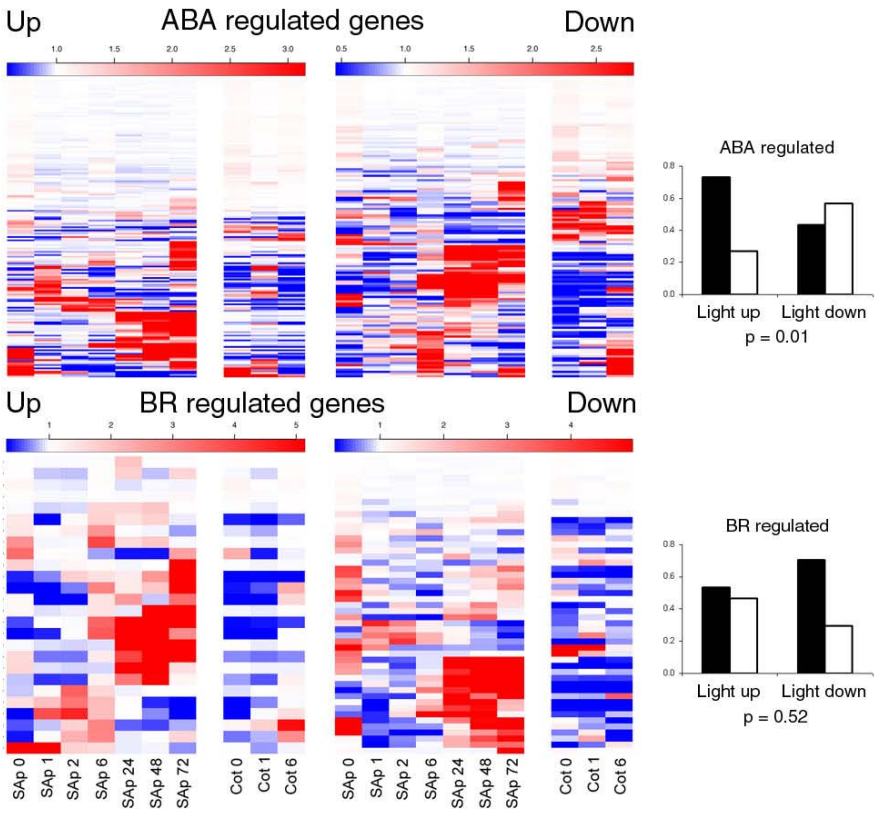

Supplemental Figure 7. Expression heatmaps for genes positively or negatively regulated by the hormones abscisic acid (ABA) and brassinolide (BR). To the right of each heatmap pair, histogram showing the proportion of genes downregulated (black bar) or upregulated (white bar) by each hormone and present in the groups of "preselected patterns" representing up- or down-regulation by light in shoot apical tissue. The p-value of a test for lack of association between the hormone and the light response is also indicated.

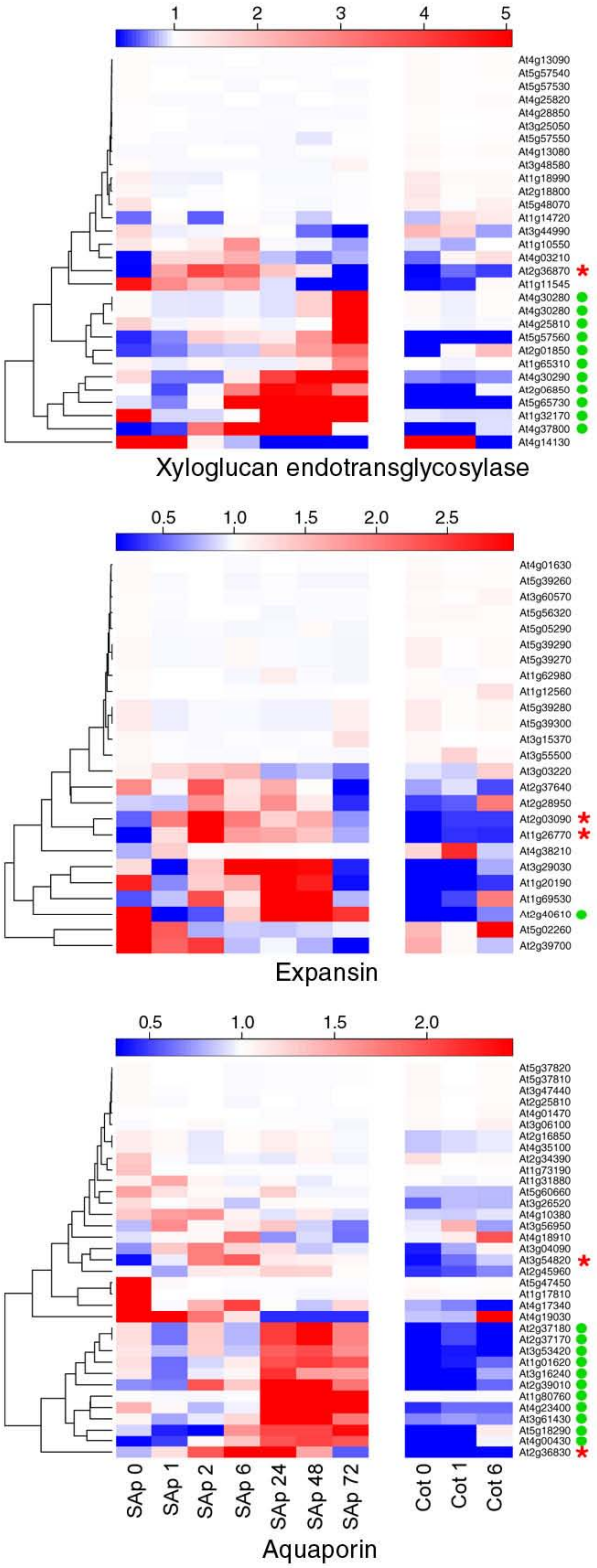

Supplemental Figure 8. Expression levels of genes encoding proteins in two families involved in cell wall modification and extensibility, and of aquaporins. Genes which were up-regulated by light rapidly, and predominantly in the meristem, are highlighted with a red asterisk. Those with late expression in the light, at the time of new leaf primordia expanding, are shown with a green dot.

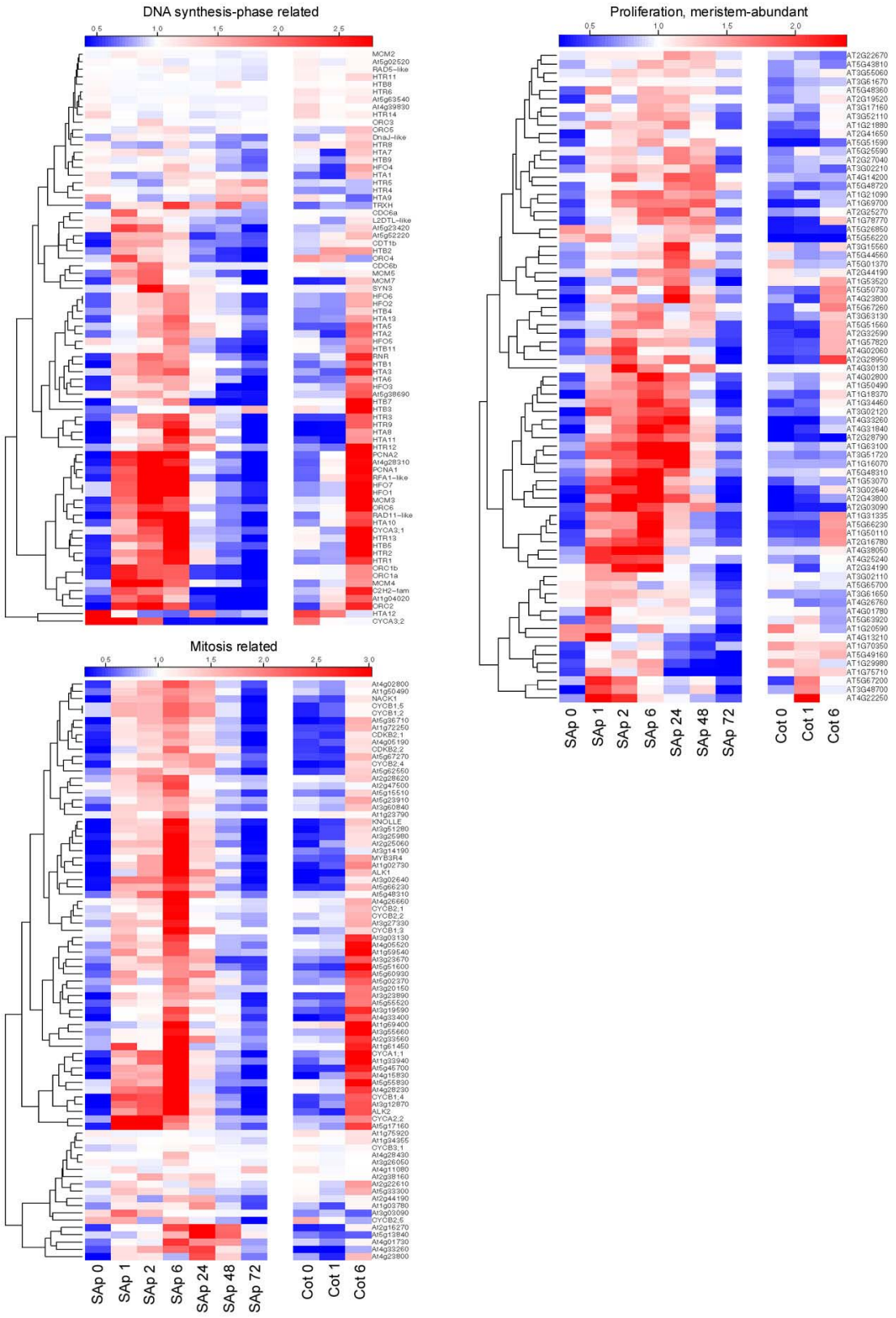

Supplemental Figure 9. Expression heatmap for genes associated with DNA synthesis phase (A), mitosis (B) or proliferation predominantly in meristems (C). Genes selected primarily from studies by Menges et al. (2005) or Beemster et al. (2005). Maximum expression was often detected at 6h. See text for details.

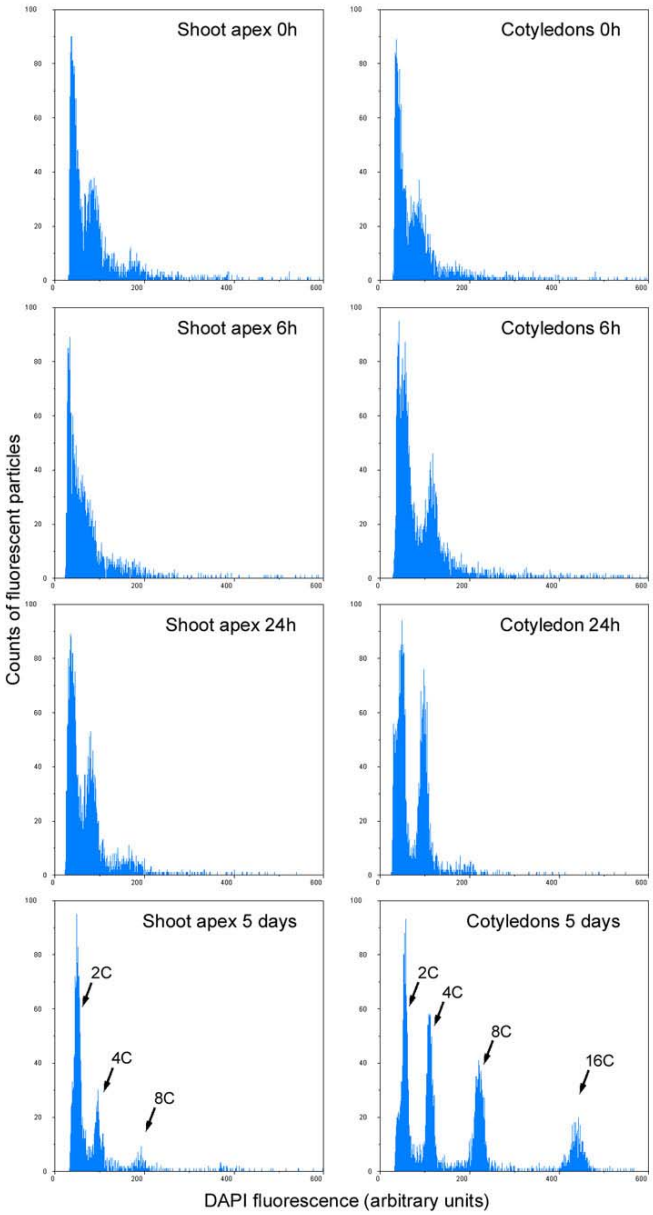

Supplemental Figure 10. Flow cytometric measurements of ploidy levels of shoot apices and cotyledons at selected time points. Samples were dissected as for the microarray analysis and counts of nuclei and their DAPI fluorescence intensity measured. In this experiment shoot apex samples show a high percentage of nuclei at the DNA synthesis phase (ploidy intermediate between 2C and 4C) and simultaneous mitosis (indicated by the disappearance of a discrete 4C peak) 6h after the transfer to light. In contrast cotyledons show endoreduplication at later times. An end-point sample (5 days after the transfer to light) is provided for illustration. The shoot apical samples show in this experiment, from time 0h, a small amount of endoreduplicated nuclei (8C) that remains constant over time, probably due to limitations in the dissection (some presence of hypocotyl hook tissue in these samples).

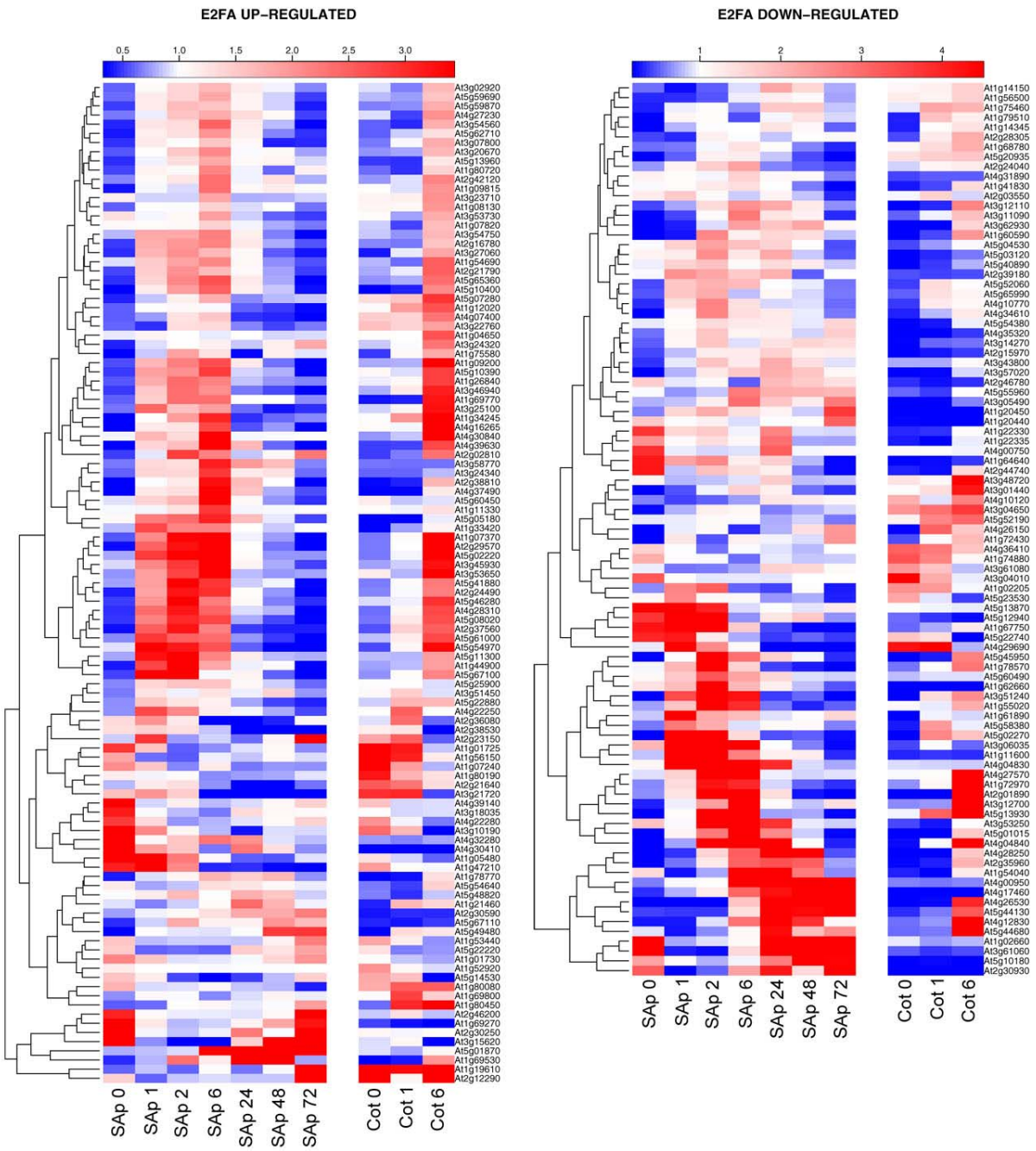

Supplemental Figure 11. Expression heatmaps for genes previously identified as positively or negatively regulated by the proliferation-promoting, differentiation-inhibiting pair of transcription factors E2FA/DPA, in the study of Vandepoele et al. (2005).

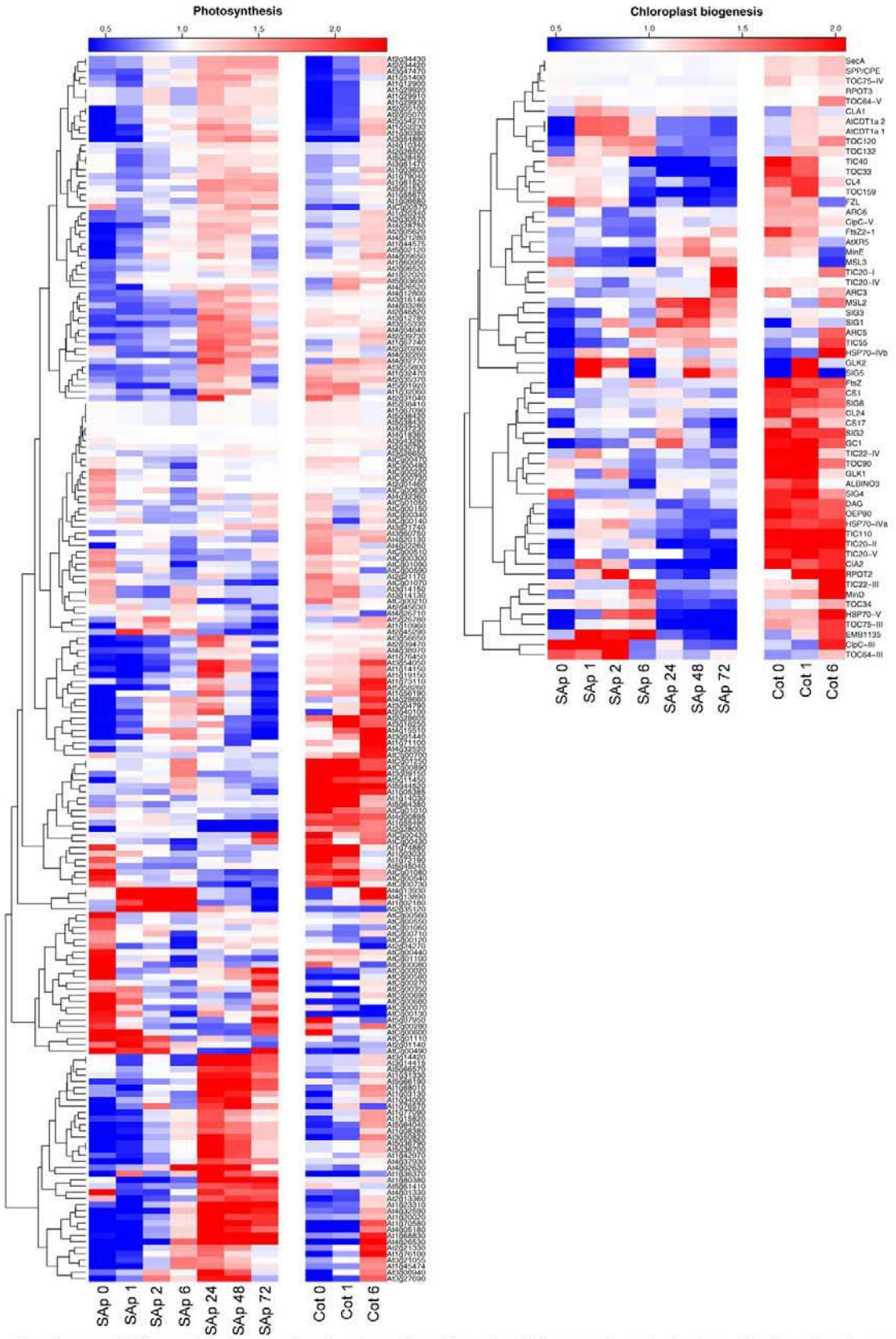

Supplemental Figure 12. Expression heatmap for chloroplast biogenesis and photosynthesis-related genes. Many were constitutively expressed in cotyledons or induced in shoot apices with expanding leaf primordia.

Supplemental Table 4. Selected overrepresented gene ontology (GO) terms within groups of differentially expressed genes following predetermined (supervised) patterns, shown in supplemental Figure 2. S: shoot apex. C: cotyledon. T: transient. Su: sustained. Lin: linear. La: late. F: flat. U: up. D: down

Pattern	Selected overrepresented GO term	p-value
STU CF	Carbohydrate metabolism	0.00020
SSuU CF	Plastid	9.6 e-09
	Cellular biosynthesis	1.2 e-06
SLinU CF	Chloroplast	6.2 e-08
SLaU CF	Thylakoid membrane	3.6 e-07
STU CTU	Transcription factor activity	1.3 e-07
SSuU CSuU	Plastid	5.5 e-08
	Defence response to pathogen	2.0 e-04
	Receptor protein signalling kinase	2.4 e-04
SLinU CLinU	Thylakoid membrane	1.7 e-07
SLaU CLaU	Oxidoreductase activity	2.6 e-03
SLinD CF	Morphogenesis	0.00027
	Development	0.00347
STD CTD	Response to hormone stimulus	0.00210
	Zinc ion binding	0.007
SSuD CSuD	Transcription regulator activity	4.0 e-12
	Response to hormone stimulus	9.9 e-08
SLinD CLinD	Ethylene mediated signaling pathway	0.00526
	Zinc ion binding	0.00040
SLaD CLaD	response to abscisic acid stimulus	1.5 e-05
	cellular metabolism	7.2 e-03

Supplemental Table 6. Primers used for quantitative real-time PCR

Gene	AGI	left	right
STM	At1g62360	GTCGGAGGACATGCAGTTTG	AAAGCATGGTGGAGGAGATG
KNAT1	At4g08150	AGAAAGCGTCACTGGAAACC	CCGAGACGATAAGGTCCATC
thylakoid protein	At3g15110	GCGTTCGGACTTCTCCTTTAC	CAATCACCTGAACTTTGATCCTC
peroxidase, cell wall	At3g49120	GAACTCCAACTCTCTGCTCCA	CATATTGGGTAAACAATTCTCACA
calmodulin-binding fam. protein	At3g49260	TTCGTCAAGTTCAGGTGGAG	CAAACCCGGTAGGACTTTGA
CHS	At5g13930	AGAGAAGATGAGGGCGACAC	ACAAGACACCCCACTCCAAC
PORA	At5g54190	ATTGGAGCTGGAACAAGACC	TCTCGCTGACTTCCCAAACT
LHCB2	At2g05100	TTGGTGTTTTATGTGAGTTTGG	TAACAGGGTGGTGTGGTTCA
GLK2	At5g44190	AATCCTCCCATCGACATTCA	CCGTCATAACACCGTCAACC
Histone *H2A*	At1g51060	CAAATTGCTTGGAGATGTGA	GTCTTCAGCAGATGGCTTGG
CYCD3;3	At3g50070	CACAGTCCAAGCAAGAAAAGG	CGACACTGAAGCAGAAGCAG
CYCB1;1	At4g37490	TCAGCAATGGAAGCAACAAG	AGCAGATTCAGTTCCGGTCA
S6RP	At4g31700	TTGAAGGAACAGCGTGACAG	GGTGACATCTTTGATTTGATTCTC
Translational activator	At1g64790	TGGGAACACACCAGTGAGAC	TCGCTTTGTTCAGGAAACTTG
TCP4	At3g15030	TCATCACCAATCCATCTCCA	GTATGCGAAAACCCGAAGAG
TCP fam. protein	At3g47620	AGGAAGAAGTGACGGTGGTG	TACTGGTTCAAGCCGGAGAG
ARR5	At3g48100	CAGCTAAAACGCGCAAAGA	CAAAAGAAGCCGTAATGTCTCA
GAI	At1g14920	TCACTGTGGTTGAGCAGGAA	ACCCAAGTAAACCTCCGACA
ATHB2	At4g16780	TTGACCATGTGCCCTTCA	AGGACGAAGAGCGTCAAAAG
TRANSDUCIN	At5g23730	CGTGAGTAGCGTCTGTTGGA	TTCTTTTGCCCACGTAAACC
HY5	At5g11260	GCTTACTTGAGCGAGTTGGA	AAGCATCTGGTTCTCGTTCTG
ACT2	At3g18780	AAATCACAGCACTTGCACCA	TGAGGGAAGCAAGAATGGAA
PIP2;8	At2g16850	GCTTCATTCCGCAGCAAC	TCCGATTACATCAAATTAAAACACA

Supplemental Methods

Preparation of shoot apex and cotyledon samples and microarray hybridisations

The dissection of shoot apex samples was carried out on seedlings harvested 0, 1, 2, 6, 24, 48 and 72 h after the transfer to light, and of cotyledon samples at 0, 1 and 6 h. Only one tissue was obtained per dissected seedling and the number of seedlings per sample ranged from ca.1500 (72 h samples) to over 4000 (0 h samples). Each sample contained material from multiple plates and several separate experiments. The whole procedure was repeated once to obtain both SAp and Cot material at 0, 1 and 6 h (biological replicates), to give a total of 16 samples. RNA was extracted using a RiboPure kit (Ambion), essentially according to manufacturer's instructions. Quality assessment of RNA, reverse transcription, synthesis of labelled cRNA and hybridisation to the *Arabidopsis* ATH1 GeneChip array (Affymetrix) was carried out by VBC Genomics Bioscience Research (Vienna, Austria). Quality control of the RNA samples was carried out on the normalized expression data, monitoring the ratios of probes for housekeeping genes at their 3' and 5' ends (Archer et al., 2006). Following identification of one noisy sample (SAp0b), a replacement third sample of SAp0 h was hybridised by the Nottingham *Arabidopsis* Stock Centre (Nottingham, UK).

Microarray analysis, supervised and unsupervised gene clustering and functional classification

Because of the limited number of replicates, the significance of the F-ratios resulting from each of the ANOVA, for each gene and interaction type, was determined by comparing it with a distribution of F-ratios computed using the bootstrap method (Efron and Tibshirani, 1993). The False Discovery Rate (FDR) was determined as a function of the resulting p-values. The FDR method was applied on those genes which had at least one expression value labeled as 'present' in the MAS5 normalisation. The distribution of the p-values was modeled using the Beta Uniform Mixture (BUM) approach (Pounds and Morris, 2003). For each normalization and interaction type, the FDR was set to 5% and the resulting threshold for the p-value determined. Genes that fell below such threshold p-value by all three normalisation methods were selected. Finally any genes that did not display at least a 2 fold change between any two

tissues or time points (or their average when available) were removed. The remaining list was considered a robust set of differentially expressed genes.

The potential involvement of hormone signaling pathways in the light response was tested through comparisons with the robust hormone-regulated genes identified in the analysis of (Nemhauser et al., 2006). Genes with the largest up- or down-regulation were selected in each case, regardless of the time after hormone application and of the potential response of the same genes to other hormones. The cut-offs of fold regulation for gene selection for different hormones were as follows: ABA (10 up at 30 or 60 min, 100 up at 180 min, 0.25 down at 30 or 60 min or 0.1 down at 180 min), auxin and methyljasmonate (10 up, 0.25 down), cytokinin, ethylene and brassinosteroid (5 up, 0.33 down) and gibberellin (2 up, 0.33 down). The cut-off values were selected to provide sufficient and, as far as possible, comparable statistical representation for all hormones. Comparisons of gene lists were carried out using online tools (Toufighi et al., 2005), and the association between the light and hormone response was measured in the relevant contingency tables using χ^2 tests.

The expression values for all of the data were clustered using the K-means algorithm based on a Euclidean distance. Each cluster was split into two by determining whether an individual gene is positively or negatively correlated with the other genes in the cluster. The K-means algorithm was implemented using the Flexclust library in Bioconductor.

As an alternative to the unsupervised clustering above, an assumption was made that the underlying expression pattern for each gene and tissue at the early time points (0, 1, 6 h) will be smooth and will adhere to one of the following models: *sustained,* where the expression level changes at an early time and then remains constant; *transient*, where the expression level changes and then returns to the original level; *late*, which is similar to the sustained except that it changes at a late time (i.e. at hour 6, rather than hour 1); *linear* where the expression level changes linearly with time and *flat*, where the expression level is unchanging. An ANOVA test for each model for each gene and tissue was applied and the model with the smallest p-value selected. In the case of the flat model, 1-p was calculated. In total, 81 patterns were collated for each tissue combination (apart from the flat model, each of the above models can be further subdivided into those that change in an increasing or decreasing manner).

For each cluster and pattern, genes were classified using two classification schemes: the Gene Ontology of the TAIR consortium was employed (Berardini et al., 2004) and a classification scheme developed for this study based on a combination of the MIPS FunCat classification (Ruepp et al., 2004) scheme and the classification developed for the MapMan microarray analysis tools (Thimm et al., 2004). The probability that a given classification occurred more or less often than expected in a given cluster or pattern was computed, using the hyper-geometric distribution.

Heatmaps were produced using code developed in R (as Bioconductor). Similarity trees between samples (supplemental Figure 1B) were calculated by the TIGR Multi Experiment Viewer (MEV). Core cell cycle-related genes were organized according to their expression using self-organising maps and 3x2 bins, in MEV.

REFERENCES

Archer, K.J., Dumur, C.I., Joel, S.E., and Ramakrishnan, V. (2006). Assessing quality of hybridized RNA in Affymetrix GeneChip experiments using mixed-effects models. Biostatistics **7:** 198-212.

Berardini, T.Z., Mundodi, S., Reiser, L., Huala, E., Garcia-Hernandez, M., Zhang, P.F., Mueller, L.A., Yoon, J., Doyle, A., Lander, G., Moseyko, N., Yoo, D., Xu, I., Zoeckler, B., Montoya, M., Miller, N., Weems, D., and Rhee, S.Y. (2004). Functional annotation of the *Arabidopsis* genome using controlled vocabularies. Plant Physiol. **135:** 745-755.

Efron, B., and Tibshirani, R. (1993). An introduction to the bootstrap. (New York: Chapman & Hall).

Nemhauser, J.L., Hong, F., and Chory, J. (2006). Different plant hormones regulate similar processes through largely nonoverlapping transcriptional responses. Cell **126:** 467-475.

Pounds, S., and Morris, S.W. (2003). Estimating the occurrence of false positives and false negatives in microarray studies by approximating and partitioning the empirical distribution of p-values. Bioinformatics **19:** 1236-1242.

Ruepp, A., Zollner, A., Maier, D., Albermann, K., Hani, J., Mokrejs, M., Tetko, I., Guldener, U., Mannhaupt, G., Munsterkotter, M., and Mewes, H.W. (2004). The FunCat, a functional annotation scheme for systematic classification of proteins from whole genomes. Nucleic Acids Res. **32:** 5539-5545.

Thimm, O., Blasing, O., Gibon, Y., Nagel, A., Meyer, S., Kruger, P., Selbig, J., Muller, L.A., Rhee, S.Y., and Stitt, M. (2004). MAPMAN: a user-driven tool to display genomics data sets onto diagrams of metabolic pathways and other biological processes. Plant J. **37:** 914-939.

Toufighi, K., Brady, S.M., Austin, R., Ly, E., and Provart, N.J. (2005). The Botany Array Resource: e-Northerns, Expression Angling, and promoter analyses. Plant J. **43:** 153-163.